University of Northern Iowa

UNI ScholarWorks

2020

A ground based investigation of snow metamorphism using an energy flux model and hyperspectral imaging across cropland, grassland and barren surface in northeast Iowa

Ayan Sasmal
University of Northern Iowa

Let us know how access to this document benefits you

Recommended Citation

A GROUND BASED INVESTIGATION OF SNOW METAMORPHISM USING AN

ENERGY FLUX MODEL AND HYPERSPECTRAL IMAGING ACROSS

CROPLAND, GRASSLAND AND BARREN SURFACE IN NORTHEAST IOWA

An Abstract of a Thesis

Submitted

in Partial Fulfillment

of the Requirements for the Degree

Master of Arts

Ayan Sasmal

University of Northern Iowa

December 2020

ABSTRACT

Snow is unstable under natural environmental conditions; it undergoes metamorphism that can be measurable with an energy flux model. The demand for snow research is increasing due to its importance for maintaining Earth's energy balance and hydrological applications. Snow metamorphism is a process of transformation of snow particles with an expense of surface free energy. Very few studies have been completed on snow metamorphism in grassland, cropland and barren surfaces that needs farther investigation. In this study, an attempt was made to measure winter snow metamorphism with physical based model and detecting snow metamorphism by using hyperspectral imaging spectroradiameter in grassland, cropland and barren surfaces.

The questions proposed in this research were: Can snow metamorphism be estimated from a ground based investigation using physical properties of snow across cropland, grassland and barren surface? Do the characteristics of snow metamorphism vary between cropland, grassland and barren surface? Can ground based hyperspectral imaging detect differences in snow metamorphism characteristics between cropland, grassland and barren surface?

The instruments used to collect field data on snow physical properties in this research were ASD FieldSpec 3 Spectroradiometer, Fluke 561 IR Thermometer, gridded mesh cards of various size, ruler, portable weighing scale, graduated measuring cylinder and magnifying glass respectively. The study indicated that by considering physical properties of snow such as, snow grain size; snow surface temperature; snow depth and snow volume coupled with meteorological parameters like, wind speed; air temperature;

atmospheric pressure and temperature at dew point derived from weather station on different days at specific time period used in an energy flux model, it is possible to measure snow metamorphism across cropland, grassland and barren surfaces. The results further showed that snow metamorphism characteristics such as: estimated amounts of snowmelt and snow grain size varied during different field days in different land types which indicate an increase – decrease in snowpack cold content respectively. Mean estimated amounts of snowmelt in grassland, cropland and barren surface found were 0.065 mm/day, 0.066 mm/day and 0.061 mm/day respectively. Diverse weather phenomenon altered the characteristics of snow metamorphism in different land types observed from this study. Results of statistical analysis with different methods showed there was no significant difference in the amounts of snowmelt between three different land types under study.

Reflectance of snow from hyperspectral imaging device showed difference in spectral signatures from different land types for different snow grain size on particular field day in specific time. After comparing all the snow reflectance spectra from three land types, the grassland showed the highest snow reflectance followed by cropland and barren surface which had the lowest snow reflectance according to different grain size on particular field day during specific time. Beside this, when PCA was applied to the combined datasets collected during different dates with ASD FIeldSpec 3 spectroradiometer it revealed components 1 and 2 with the following hyperspectral bands with component loading > 0.9: 1014.5, 1024.5, 1034.5 and 355, 356, 374.5 and 394.5 nm

at wavelength range between 350nm – 1039nm bands were important for identifying snow metamorphism characteristics .

Additional instances of snow metamorphism were observed from this study such as, icy structures in three different land classes on a particular day with varied amounts of snowmelt and grain sizes that require further investigation. During icy condition the estimated amounts of snowmelt found in three different land types as, cropland: 0.0536 (mm/day); grassland: 0.0544 (mm/day) and barren surface: 0.0491(mm/day) having snow grain size .5mm, 1mm and 2mm respectively.

This study provided valuable insights about snow surface energy balance regulation and its effect on seasonal snow metamorphism in cropland, grassland and barren surfaces respectively. The importance of hyperspectral imaging spectroradiometer in detecting snow metamorphism was determined. Snow spectral libraries were created according to grain size, which can serve as future references for corresponding studies on snow metamorphism in three different land classes under study respectively.

A GROUND BASED INVESTIGATION OF SNOW METAMORPHISM USING AN

ENERGY FLUX MODEL AND HYPERSPECTRAL IMAGING ACROSS

CROPLAND, GRASSLAND AND BARREN SURFACE IN NORTHEAST IOWA

A Thesis

Submitted

in Partial Fulfillment

of the Requirements for the Degree

Master of Arts

Ayan Sasmal

University of Northern Iowa

December 2020

This Study by: Ayan Sasmal

Entitled: A GROUND BASED INVESTIGATION OF SNOW METAMORPHISM

USING AN ENERGY FLUX MODEL AND HYPERSPECTRAL IMAGING ACROSS

CROPLAND, GRASSLAND AND BARREN SURFACE IN NORTHEAST IOWA

has been approved as meeting the thesis requirement for the

Degree of Master of Arts

Date	Dr. Andrey N Petrov, Chair, Thesis Committee
Date	Dr. Alan Czarnetzki, Thesis Committee Member
Date	Dr. Bingqing Liang, Thesis Committee Member
Date	Mr. John DeGroote, Thesis Committee Member
Date	Dr. Jennifer Waldron, Dean, Graduate College

ACKNOWLEDGEMENTS

Throughout developing and writing of this dissertation, I have received a great deal of support and assistance from all my advisors.

First and foremost, I would like to thank my advisor, Professor Andrey N Petrov, whose expertise was invaluable in formulating the research questions and methodology. His insightful feedback pushed me to sharpen my thinking and brought my work to a higher level. And also his support during my entire MA study was very useful.

I would like to express my sincere gratitude to Professor Alan Czarnetzki for his continuous support to my research. I admire him for his patients, motivation, enthusiasm, and immense knowledge. His guidance helped me all the time during this research and writing of this thesis.

I would like to thank Professor Bingqing Liang for her invaluable suggestions and guidance throughout this research. Her early insights lunched the greater part of this dissertation. She provided me with the tools that I needed to choose the right direction and successfully complete my dissertation.

I would like to thank Mr. John DeGroote for his suggestions and encouragement in writing the thesis which was extremely valuable. His insightful comments, hard questions and moral support had made it possible to complete this dissertation successfully.

I would also like to thanks Professor Jennifer Waldron and Professor Patrick Pease for their support in doing this thesis. Acknowledgement is extended to University of Northern Iowa, Department of Geography for fulfilling my dream of being a student here and providing me funds to conduct this research.

Finally, I would like to express my special appreciation to my family members for their moral support and continuous encouragement throughout my years of study and through the process of researching and writing the thesis.

Author

Ayan Sasmal

TABLE OF CONTENTS

LIST OF TABLES

LIST OF FIGURES

CHAPTER 1

INTRODUCTION

1.1. Background of the Study

Snow forms in the cloud when the temperature falls below 0°C in the presence of super cooled water and suitable aerosols (cloud condensation nuclei) (Pomeroy & Brun, 2001). The variability of snow morphology is very high when it falls and after it makes the ground cover (Colbeck, 1987). Similar to the rainfall that directly recharges groundwater and stream runoff accumulated snow on the ground creates a temporary fresh water reservoir that gets released after melting triggered by rising temperature (Lopez et al., 2020). Melting of snow can be a factor for risks to the society by causing avalanches (Schweizer et al., 2003) and widespread flooding either directly with rapid increase in temperature (Merz & Blöschl, 2003) and rain-on-snow events (Sui & Koehler, 2001) or indirectly through dam failure accidents (Rico et al., 2008). In contrast, snow cover ground is vital for both ecological reason and for many human activities such as: hydropower generation, tourism and agriculture purpose (Barnett et al., 2005). Therefore, snow is an important component of Earth water cycle both in mountainous areas as well as in many mid and high latitude areas. Complexity of snow coupled with the limited data availability has led to the development of various models to improve its understanding to support management practices among which physical based model like the energy flux provide the best representation of this process with the toll of high data requirement (Lopez et al., 2020). To date, few studies have been completed about snow metamorphism in different land surfaces. Most studies using snow energy flux models on

seasonal snow pack was done at low elevation areas either in forested areas or on glaciers or on sea ice (Kuusisto, 1986). The present study is devoted to measure snow metamorphism using an energy flux model and detect it with the application of hyperspectral imaging across cropland, grassland and barren surface respectively. Snow metamorphism is defined as an endless process of transformation of snow crystals occurs inside snowpack from sublimation and deposition of water vapor includes physical factors such as: pressure, temperature and temperature gradient that evolves snow particle (Wen et al., 2014; Fabienne, 2012; DeWalle & Rango, 2008).

1.1.1. Role of Snow on Earth.

Snow is an important natural resource (Negi & Kokhanovsky, 2011) that influences regional as well as global climate (Negi et al., 2015; Lee et al., 2017). It is a vital element of the cryosphere and the climate system (Langlois et al., 2014). The global radiation balance gets affected by the snow cover albedo (Fabienne, 2012). Snow albedo is defined as the sum of the fraction of incoming radiation reflected back by the surface of the snow to every direction in the sky (Riihela et al., 2011). Basically, snow albedo depends on physical and chemical state of snow which constantly evolves during the melting season (Kuusisto, 1986; Choudhury & Chang, 1981). Melting of snow and ice on the ground serve as a significant portion of the Earth's fresh water and are crucial for hydrological cycle in various regions (Greene, 2007), particularly in the Northern Hemisphere which is normally covered with seasonal snow every year (Langlois et al., 2014).

Land snow acts as an interface between land surface and the atmosphere that tends to control the conductive and radiative exchanges between those two (Male & Granger, 1981; Brun et al., 1989; Gustafsson et al., 2001). The geophysical and thermophysical properties of snow were considered to be sensitive to climate variability and changes crucial for the hydrological and climatological processes on earth respectively (Rango, 1980; Schultz & Barrett, 1989; Albert et al., 1993). Due to the dynamic property of snow, any changes in snow is very important to understand for providing insights about changes in the elements of the cryoshpere, earth's energy balance, climate change and water resource management in several regions.

In the USA, western states experience earlier snowmelt that gets discharged in the snow occupied river system (Stewart, 2009). For instance, runoff in Colorado River headwaters were mostly generated due to spring-summer snowmelt from high elevated (>2800m) forested and alpine areas (MacDonald & Stednick, 2003). Rising western population will let the demand for water usage in the United States increase (Kinar & Pomeroy, 2015). In contrast, earlier snowmelt can acts as a key driver of hydrological hazards like the spring floods, summer droughts and rain-on-snow (ROS) events (Chen et al., 2015; Blöschl et al., 2017; Freudiger et al., 2014). Therefore, a correct knowledge about the amounts of water availability from snowmelt and the timing of run-off can aid in managing water sources in those regions (Bryant & Painter, 2010; Harshburger et al., 2005).

Melting of snow causes disastrous floods in many parts of the world that can results in the loss of life, property and infrastructure damage, agricultural losses and it

could be a reason for national disruptions to transportation (Usul & Turan, 2006; Andresen et al., 2012). For instance, in past damaging flood caused by rapid melting of snow and rain-on-snow (ROS) (Marks et al., 1998; Sui & Koehler, 2001) on the Red River in Manitoba and North Dakota (Pomeroy et al., 2007) had heavily impacted daily life there and its surrounding environment (Kinar & Pomeroy, 2015). Unusual wet winter and spring in Iowa of 2007 to 2008 had created an exceptionally wet precursor conditions from heavy discharge that took place at more than 60 streamgage location in the eastern Iowa (Buchmiller & Eash, 2010). In the year 2019, a newspaper reported that melting of snow, rainfall and frozen flood gates has damaged the city in Northern Cedar Area of Cedar Falls (Forbes, 2019).

Modeling accumulation of snow and snowmelt is not only important for maintaining water balance for runoff, local water availability and groundwater recharge particularly in the middle and high latitudes on a regional scale (Zeinivand & de Smedt, 2009; Akyurek & Sorman, 2002; Jain et al., 2008). It can also contribute to control damaging flood cause by snowmelt in several regions. Thus, snow serves an important component for hydrological applications as well as it is also sensitive to climatic change (Singh et al., 2005).

1.1.2. Snow and its Properties

To understand the properties of snow it is of prime importance to know about the science behind the formation of snowflakes in the clouds (Fabienne, 2012). Initially the process starts when particles of ice in the clouds get nucleated with aerosols (salts, dust and fine particles) which later increases from vapor deposition, aggregation (collision of

ice particles) and riming (collision with super cooled water droplets) (Pruppacher & Klett, 1996) and then falls down from the sky as snow crystals or snowflakes. The shape and size of the snowflakes varies greatly due to the factors such as: temperature, degree of super saturation of water vapor and humidity which ultimately bounds to cluster and transform into snowpack (Fabienne, 2012; Pirazzini et al., 2015). After the snow gets deposited, the land cover changes the properties of snow that undergoes complicated interactions with the landscape and different atmospheric conditions (Langlois et al., 2014; Muñoz et al., 2013). So understanding snow microstructure can help in physical modeling of snow and developing remote sensing algorithms to detect snow metamorphism (Leppanen et al., 2015). The microstructure of snow can be studied either through static observations of snow grains or in detail under microcomputed tomography (μCT) (Fabienne, 2012).

Studies on microstructure of snow reveal that typically snow particles are porous granular medium composed of ice crystals and pore space in it, and at a specific temperature below 0 degree Celsius the snow particles gets filled up with air and water vapor to form dry snow, however, when the temperature rises above 0 degree Celsius the pores in the snow contains additional liquid water to convert into wet snow (Endrizzi, 2007). Aging causes decomposition in snowflakes which results in considerable amount of variation in snow reflectance by decreasing its albedo strength and timing of snowmelt (Flanner & Zender, 2006). The snowpack albedo depends on the single scattering property of the individual snow crystals of various shapes and sizes that frequently bounds in clusters (Pirazzini et al., 2015).

Besides snow albedo gets affected by the synoptic scale warming which coarsens the snow grain size, there are additional anthropogenic source that decreases the snow albedo significantly are the light absorbing impurities such as, the dust particles and shoots (Hansen & Nazarenko, 2004; Painter et al., 2005), that finally alters the snowpack energy balance over the snow surface (Nolin & Stroeve, 1997). To compute the energy flux in snowpack four principal components of weather were considered such as incident solar radiation; incident long-wave radiation; air temperature; relative humidity and wind speed respectively (Cline et al., 1998). Among those components in maximum cases shortwave and long-wave radiation components were most likely to dominate the energy balance which varies considerably from one area to another (Boudhar et al., 2016). The majority of energy balance studies in various locations specified that net radiation commonly contribute to about 50 to 90 percent of the energy required for snowmelt (Male & Granger, 1981; Willis et al., 2002; Mazurkiewicz et al., 2008). Therefore, an effective way to determine snow metamorphism is by computing the net surface energy flux in snowpack (Hong et al., 1992) for estimating the amounts of snowmelt at individual station respectively.

1.1.3 Remote Sensing of Snow

Remote sensing is defined as an art and science of obtaining information about an object from a distance without actual contact of the object. Most researches on snow were carried out through remote sensing (Saha et al., 2019) because physical measurement of snow characteristics are highly expensive and climate change impose change in snow characteristics at a regular interval (Lundberg et al., 2008). Therefore, remote sensing

tends to be a very effective way to quantify snow metamorphism. Remote sensing potentially offers the ability to quantitatively examine the physical properties of snow (Nolin, 2010) and thereby, can able to predict the time of snowmelt. Optical remote sensing of snow from satellites imageries were limited in the capability to determine properties such as: snow depth, snow cover, snow quality and snow water equivalent (SWE) because physical properties were not directly measured (Dozier, 2011; Saha et al., 2019). Snow water equivalent is the amount of water content within the snowpack. Collection of field spectrums from high resolution spectroradiometers were used to provide the data required for radiometric and atmospheric correction and validation of airborne and satellite imagery for remote sensing of snow properties (Curtiss & Goetz, 1994; Clark et al., 2002; Milton et al., 2009), which can also be used as a ground based mechanism to calibrate a variety of sensors (Kuester et al., 2001). Due to an increasing demand on quantitative data for various application and since snowpack properties varies widely both in time and space, both satellite retrieved and ground-based measurements have not meet the demand yet (Lundberg et al., 2008). Therefore, this study intends to derive information about snow metamorphic characteristics in cropland, grassland and barren surface from ground based investigation using an energy flux model and hyperspectral imaging spectroradiometer data for future contribution in snow research on a regional scale.

Hyperspectral remote sensing is a technique of measuring reflected radiance into narrow contiguous spectral bands over the full visible and solar reflective infrared spectrum (Goetz et al., 1985). Hyperspectral remote sensing data classifications are based

on the spatial structures derived with morphological and quality profiles (Marpu et al., 2012). Invention of highly sophisticated spectroradiometers like the ASD FieldSpec® allows to analyses the amount of energy transferred from an object's numerous natural processes which can be observed from the principle domain of solar radiance roughly between 350nm and 2500nm spectral wavelength (Danner et al., 2015). Therefore, in many applications ASD FieldSpec® was found to be very useful for detection, identification and quantification of materials on the Earth's surface due to its ability to collect reflected light from an object using its very high number of contiguous spectral bands (Salisbury, 1998; Curtiss & Goetz, 1994). Creating precise libraries of spectra of specific materials from spectroradiometer data can greatly improves the accuracy of resulting interpretations and classifications of an object from remote sensing perspective (Garfagnoli et al., 2013). Earlier estimating the properties of hydrologic and Climate models from imaging spectrometer data were principally used to understand the relationship between snow's physical properties and the resulting electromagnetic signal (Dozier et al., 2009). This study aims to relate the characteristics of snow metamorphism with the spectral reflectance data of snow to detect snow metamorphism in three different land classes: cropland, grassland and barren surface under natural environmental condition to check the sensitivity of the hyperspectral imaging respectively. For doing this, an energy flux model was used to estimate amounts of snowmelt at different stations in three different land types on different days. Then the estimated amounts of snowmelt according to snow grains size were matched with the snow reflectance data taken on different field days using spectroradiometer to detect snow metamorphism. Finally,

spectral libraries were created with respect to snow metamorphism characteristics. Because spectra collected from the surface are important for fundamental research in remote sensing and the corresponding spectral libraries has been a conventional way to represent it both domestically and internationally (Clark et al., 1993; Zhang et al., 2017). Therefore, this research will add new knowledge to the field of hyperspectral remote sensing science in respect to snow metamorphism across three different kinds of land types such as, cropland; grassland and barren surfaces respectively.

Also, information about additional observable characteristics of snow metamorphism like melt-freeze metamorphism or ice-crust structure found in cropland, grassland and barren surfaces were recorded for the purpose of future study. Melt-freeze metamorphism is defined as a process that modifies the icy crystals in deposited snow formed due to the wetting of grains by melt water followed by freezing combined with accelerated equitemperature metamorphism that consequently increases the density and strength of snowpack (Singh et al., 2005). And ice-crusts potentially develop from freezing of wet snow layer after releasing its latent energy (Colbeck & Jamieson, 2001), generally occur when the percolated water from rain-on-snow (ROS) gets accumulated and a significant amount of that water at the bottom of the snowpack re-freezes (Riseborough et al., 2008; Weismüller et al., 2011).

1.2. Research Goal

The goal of this study was to develop a scientific approach with an integrated methodology that includes an energy flux model and hyperspectral imaging spectral reflectance of snow to detect characteristics of snow metamorphism like snow grain size

and amounts of snowmelt across grassland, cropland and barren surface in Northeastern Iowa. Finally, to develop spectral libraries according to snow grain size with the reflectance spectra from snowpack collected in the field with high resolution ASD FieldSpec 3 spectroradiometer.

1.2.1. Research Questions

i. Can snow metamorphism be estimated from ground based investigation using physical properties of snow across cropland, grassland and barren surface?

ii. Do the characteristics of snow metamorphism vary between cropland, grassland and barren surface?

iii. Can ground based hyperspectral imaging detect differences in snow metamorphism characteristics between cropland, grassland and barren surface?

1.2.2. Research Objectives

a. Collecting the physical properties and spectral reflectance of snow from field.

b. Quantifying snow metamorphism in winter based on field measurements of snow properties to calculate the net surface energy change (NEC) in snowpack for estimating the amount of snowmelt at different phases of snow metamorphism under natural environmental condition in cropland, grassland and barren surfaces.

c. Comparing the snow metamorphism characteristics between the three different land classes.

d. Relating the snow metamorphism characteristics to hyperspectral imaging spectra of the snow reflectance and detecting the difference in the spectral reflectance of snow collected from ground based hyperspectral imaging spectroradiometer.

<p style="text-align: center;">1.3. Hypothesis</p>

Snowpack evolution is a continuous process, whether there will be difference in the characteristics of snow metamorphism between three different land types such as cropland, grassland and barren surface with time is unknown to us. Therefore, my aim is to determine snow metamorphism and to find the differences between snow metamorphism characteristics between three different land classes that can contribute valuable insights in snow research. To see if there is difference in snow metamorphism in between three different land classes I proposed my hypothesis to be: the estimated amount of snowmelt will be statistically significant across the three different land cover types. Here both one-way ANOVA and t-test analysis methods were used to test the hypothesis respectively.

<p style="text-align: center;">1.4. Significance of the Study</p>

A good model for detecting snow evolution could help us to improve our understanding of snow metamorphism in different land cover types. It could be useful for future research works to understand the complex reaction taking place inside snowpack. Moreover, the assessment of the utility of hyperspectral imaging in doing this can greatly improve our ability to gather and analyze data on snow metamorphism in three different land classes under study. This study will also provide insights about winter snow metamorphism in three different land classes such as, grassland, cropland and barren surface which could be beneficial for snowmelt water management purpose. The insights will be useful particularly for understanding snow surface energy balance regulation and its effects on snow metamorphism on different land types. Indirectly, the findings from

this study can also be beneficial for developing snowmelt flood prediction models and motivate investigation of such factors influencing the evolution of snowpack across different land surfaces. The final outcome from this study, spectral libraries of snow metamorphism across three different land classes with respect to snow metamorphism characteristics will be promising to serve as future references for corresponding studies on seasonal snow metamorphism in cropland, grassland and barren surface respectively.

1.5. Structure of the Chapters

This investigation aimed to understand winter snow metamorphism from physical based model and detecting it through hyperspectral imaging respectively. In Chapter 1, I have described snow and its importance on Earth, effects of snowmelt, two different approaches to quantifying snow metamorphism such as, remote sensing approach to detect snow metamorphism and energy flux model to determine snow metamorphism, problems associated with current researches, proposed research questions, hypothesis and significance of this study. Chapter 2 discusses the literature related to snow metamorphism, two approaches to study metamorphism and gaps in those studies and lastly land types distribution in the USA. Chapter 3 and 4 is about the proposed methods used in this study, analysis of data and interpretation of the results. Chapter 5 contains discussions, conclusions, limitations and future direction of this research.

CHAPTER 2

LITERATURE REVIEW

On Earth snow cover plays an important role both globally and regionally by keeping the Earth's radiation budget in balance (Klein et al., 2000; Jain et al., 2008; Zhao & Fernandes, 2009). Snow is also a key element of Earth's hydrological cycle and it balances the surface energy (USACE, 1956; Mote et al., 2018; Frei et al., 2012). As for instance, snow from the Arctic (Marsh, 1990) and Canadian Prairies together can contribute up to more than 80% of water to its streams (Barnaby, 1980; Gray & Landine, 1988; McKay & Blackwell, 1961). During the mid-winter time about 40–50% of the Northern Hemisphere approximately is covered with snow (Hall et al., 1995; Pepe et al., 2005; Lemke et al., 2007). It is important for availability of local water supply, river run-off and groundwater recharge at middle and high latitudes (Akyürek & Sorman, 2002; Jain et al., 2008). Beside this, wintertime snowpack acts as an insulator for the local environment and provides an insulating cover for vegetation and hibernating animals (Seibert et al., 2015). Simultaneously, snowmelt significantly acts as surface water input for various hydrology processes (Tarboton et al., 1995). Seibert et al. (2015) after studying snow and ice on hydrosphere found in many places the dry season snowmelt water contributes to irrigation, industries and households, whereas, the cold seasonal snow acts as a temporary storage component for river runoff and water supply regimes. Callaghan and Johansson (2014) found that snowmelt is a potential source of soil water for growing vegetation during springtime. Therefore, correctly predicting snow melting is important for economic, social and ecological reasons and particularly when melt water is

crucial for sustaining summer base flows that ensures the availability of irrigation water for summer crops and trees (Boudhar et al., 2016). Prediction requires real-time information about snowmelt that causes run-off for water resource management, irrigation, flood prediction and hydropower production respectively (Vikhamar & Solberg, 2003).

Due to the change in northeastern United States winters in several decades, shallower snowpack, fewer days of snow cover and increase precipitation in the form of rain during winter were observed (Adolph et al., 2017). Rise in winter precipitation, temperature (McCarthy et al., 2001; Karl & Trenberth, 2003; Benestad, 2005) and rain-on-snow (ROS) events has been found to have greatly increased (Rennert et al., 2009; Liston & Hiemstra, 2011) including in the Arctic from last few decades (Serreze et al., 2009; Derksen & Brown, 2012). Haeberli and Whiteman (2015) observed snow can interact with almost everything on Earth and it was greatly variable in space and time since it depends on short-term weather condition like precipitation and temperature which made it easily eroded, transported and re-deposited by wind energy. Basically, alteration in snowpack has consequences on its surrounding environment and upon people that led to the development of several scientific ways to continuously monitor snow cover on Earth and measure how much of the planet is covered by snow (National Snow and Ice Data, 2020).

2.1. Seasonal Snow Cover

Seasonal snow is define as the snow that accumulates during particular season, it covers nearly 47 million km^2 or 30% of the total Earth's total land surface among which

the Northern Hemisphere contains the maximum snow cover mainly found along the parts of North America and Eurasia (Brodzik & Armstrong, 2017; Robinson et al., 1993). Together North America and Eurasia gets covered with more than 50% of seasonal snow (Beria et al., 2018) every year. In the western United States snowmelt supplies large quantities of water to its rivers (Daly et al., 2000; Marks et al., 2001; Rice et al., 2007), particularly in the states of Oregon (Harr, 1981), Washington (Koch & Fisher, 2000; Pelto, 2004), Colorado (Fassnacht et al., 2001), and California (Davis et al., 1999). Snow cover also acts as heat storage that supplies a good quantity of heat energy during the process of its phase change or sublimation (Rasmus, 2005). Being heterogeneous in time and space, seasonal snow cover and its melt regimes need to be described and modeled to understand phenomenon like runoff, ground temperatures or slope movement respectively (Schmid et al., 2012).Seasonal snow in the Northern Hemisphere is closely linked to the global radiation balance (Haeberli & Whiteman, 2015). Snow cover, snow albedo and snow water equivalent (SWE) directly impact the environment, water availability and economics of a place (Seidel et al., 2016). SWE is the quantity of liquid water obtained upon complete melting of the snowpack per unit ground surface area (Seibert et al., 2015).

Saha et al. (2019) studied the composition of snow and found pure snow was composed of small crystalline ice particles formed from snowflakes dropped from cloud. Singh et al. (2005) added to it by saying snow was made up of ice composed of small, white or translucent, delicate, often branched or star-shaped hexagonal (tabular or prismatic) crystal of frozen water produced directly from sublimation of atmospheric

water vapor around solid nuclei at a temperature below the freezing point. So to measure grain size in seasonal snow in field condition Nolin and Dozier (2000) used gridded card and magnifying lens for remotely sensing grain size of snow with hyperspectral method. Rasmus (2005) observed snowpack was formed of an ice skeleton embedded with liquid water and moist air in its pores which slightly alters in case of seasonal snow cover where a large portion of its volumetric contents always air. The layers formed in the snowpack are caused due to deposition events and metamorphic processes (Pielmeier & Schneebeli, 2003). Later in a study by Wen et al. (2014) on snowpack layers suggested under natural environmental condition snow metamorphism undergoes five stages of evolution: i) unstable kinetic metamorphism at the surface; ii) unstable kinetic metamorphism under pressure; iii) stable kinetic metamorphism; iv) equilibrium metamorphism; and v) wet snow metamorphism. Dingman (2015) indicated, an alteration in the snowpack take place with snowmelt over time that consists of three identical phases: (a) the warming phase, (b) the ripening phase, and (c) the output phase. During melting air from the snow cover gets displaced by increasing its density and the average liquid water content in the snow layers (Sensoy et al., 2006). High average temperature and more absorption of solar radiation potentially increase the thermal state of snowpack responsible for its rapid densification (Datt et al., 2008).

2.2. Snow Energy Flux Model

Coakley (2003) found the reflectance and albedo of snow surface radiation not reflected back gets absorbed by the snow that increases its surface temperature, evaporates water melts and sublimates snow and ice, and energizes the turbulent heat

exchange between the surface and the lowest layer of the atmosphere. Dutta et al. (2015) reported the main driving force of the earth's atmospheric system was the energy balance structure. They concluded the exchange of energy and matter was one of the most challenging fields of research in global climate change. Lu et al. (2016) then compared the snow surface energy exchange from different years at the same locations suggested it was useful for understanding the influence of climate change on snowmelt. Adolph et al. (2017) found snow cover acts as a major control over the surface energy budget in temperate regions due to its high reflectivity compared to underlying surfaces. The exchange of energy between the land surface and atmosphere gets modified from snow which significantly affects the distribution of heating in the atmosphere by altering the surface albedo and regulating turbulent heat and momentum fluxes at the surface (Sensoy et al., 2006).

Therefore, a correct model of snow metamorphism is crucial for modeling climate as well as for hydrologic applications (Chen et al., 2014). Snow energy flux model has been greatly used in spatial context for hydrological, hydrochemical and geomorphological applications (Kirnbauer et al., 1994). For instance, Negi et al. (2004) used snow surface energy balance model to estimate snow melt in seasonal snowpack. Cline (1997) studied snow surface energy exchange and snowmelt at a continental mid-latitude Alpine site during spring season and found net radiative flux and net turbulent flux provides 75% and 25% of the total energy required for snowmelt. Datt et al. (2008) in a study to describe time series analysis of snow-melt, radiation data and energy balance for a seasonal snow cover at Dhundi field station of SASE, which lies in Pir

Panjal range of the N–W Himalaya, found net radiation energy was the main component of snow surface energy budget responsible for snow melt. Zhao et al. (2013) argued that for calculating snow surface energy flux three fundamental factors were needed: snow albedo, snow grain size, and snow temperature. Snow reduces its surface free energy at a constant rate by evolving into denser and larger grain size which could be understood in the light of phase-equilibrium thermodynamics and crystal growth phenomenon (Colbeck, 1987).

The two most important processes that affect snow surface energy change are radiative and turbulent heat transfer (Cline, 1997). And ground and advected energy from the rainwater are less frequent or negligible (Obled & Harder, 1979; Male & Granger, 1981). However, snowpack and environment are constantly interacting with each other results in energy exchange between atmosphere and the below ground (Datt et al., 2008). But interestingly the temperature distribution within the snowpack is fixed by the process of energy exchange responsible for timely metamorphic changes in snowpack (Colbeck, 1983).

2.3. Remote Sensing of Snow with Hyperspectral Imaging System (HIS)

Dimopoulos (2017) described remote sensing as a technique for collecting data and information acquisition about an object, area or a phenomenon without an actual contact. Hyper-spectral imaging systems use hyper-spectral sensor and proper software to analyze data and represent a major breakthrough in remote sensing. Lundberg et al. (2008) identified remote sensing techniques including satellites, airplanes and unmanned flying vehicles operations that had the advantage over ground-based techniques by

covering much larger areas but possess lower accuracy and were still dependent on ground-based techniques for validation. Clark (1999) argued that all substances consist of their own characteristic spectrum which could be detected through sensors. Richards (1999) found hyperspetral imaging sensor at a particular spatial resolution were capable of offering high spectral resolution to minimize missed detection and maximize accuracy of detecting snow particles. O'Brien and Munis (1975) observed snow possesses a distinctive spectral signature (very high reflectance in the visible region) compared to other land features. So it is a very common practice in spectral analysis to relate the morphological features of the spectra with different materials absorption response (Clark & Roush, 1984; Green & Craig, 1985).

Spectral analysis has both advantages and disadvantages for snow detection. For instance, Nolin (2010) found that with advancements in remote sensing technique it began to offer local, regional and global observations of seasonal snow thus providing key information on snowpack processes. In contrast, the drawback of snow spectra is the strong influence of the position of the features on the background can cause difficulties in identifying and quantifying the material of interest if the spectra are not properly pre-processed (Jaoumot et al., 2005; Ye et al., 2008). Coakley (2003) found snow surface albedo was a key ingredient in remote sensing of snow top. It depends upon the wavelength, zenith angle, snow grain size, impurity content and cloud cover, and it was very important for measuring snow melting and snow energy balance at the surface (Warren, 1982).

Villa et al. (2011) indicated advantage of hyperspectral remote sensing was that it provides detailed spectral information which facilitates detection, classification of surfaces and chemical elements from the observed image, whereas, its drawback was its low spatial resolution varies only up to few tens of meters. Dozier and Painter (2004) modeled the properties of snow in the Alps found both multispectral and hyperspectral remote sensing techniques could be useful for retrieving properties like grain size, contaminants, temperature, liquid water content, and depth or water equivalent of snowpack. Since from the past two decades substantial attention has been given to examine the relationships between snow grain size, snowpack energy balance and snow albedo (Nolin & Dozier, 2000), therefore, in this research I have attempted to create a relationship between snow metamorphism characteristics with snow reflectance in cropland, grassland and barren surface and detect it using hyperspectral imaging respectively.

O'Brien and Munis (1975) and Bolsenga and Kistler (1982) found reflectance of fresh snow generally varies more in the red end of the visible spectrum which declines in the shortwave infrared region (SWIR) at 1700 nm where there were minor peaks at approximately 1090–1100 nm. Wiscombe and Warren (1980) also observed the same kind of minor peak in the reflectance spectra of snow at different wavelengths between 1830nm to 2240 nm with a strong depression of reflectance from 1950 and 2050 nm wavelength which was later explained by Warren (1982) in a study on contaminated snow. Singh et al. (2005) observed strong reflectance of snow in visible region of the wavelength that decrease gradually and becomes insignificant in SWIR region. Minor

peaks were found near 1100nm, 1300nm, 1800nm and 2200nm wavelength with a strong depression near 1950nm and 2050nm wavelength. The NIR showed reduction in peak which was centered at 1050nm and 1350. They also found with the increase in grain size of the snow the spectral reflectance of snow deceases considerably the lowest was at 7 and < 8 with 1-2 mm grain size followed by < 1mm grain size at 8 and < 0.5mm grain size at < 9.

Research conducted to identify the spectral properties of snow by Negi et al. (2015) and Saha et al. (2019) found that wavelengths 550nm, 1240nm and 1660 nm were useful for identifying different snow features. Dozier et al. (2009) argued snow reflectance in the visible spectrum gets degraded by contaminants such as dust, algae and soot. Singh et al. (2010) analyzed their snow reflectance data collected from spectroradiometer at Beas basin in Pir Panjal range at 2000-4000m height found band absorption depth at 1025nm increases with the increase in snow grain size. In their research they considered the snow grain size as fine (<0.5mm); medium (1mm) and coarse grain (1-2mm). To understand the effect of contamination and mixed objects on snow reflectance Negi et al. (2006) conducted a field experiments in the upper Indian Himalaya during the winter seasons of the years 2004–2005 and 2005–2006 observed that as the amount of contamination increases the peak of snow reflectance in the visible region gets shifted toward the higher wavelength range i.e., towards SWIR region.

Since very little is known about snow metamorphism on different land types such as, cropland, grassland and barren surface, for understanding snow metamorphism characteristics across those land types both *in-situ* measurement of snow physical

properties and hyperspectral imaging was used to detect snow metamorphism that could be very useful and also very promising method for future research on snow.

<center>2.4. US Land Cover Characteristics</center>

A total of 2.3 billion acres of the U.S. land according to 2012 data 392 million acres were occupied by cropland, 655 million acres land were under pasture and range, 130 million acres was grazeland and 8 million acres were farmsteads and farm roads (Bigelow, 2017). Chamberlain and Tighe (2009) and Homer et al. (2007) demonstrated that, data about land cover types were valuable and often very crucial product for performing studies and analysis in different fields such as scientific, economic and governmental applications for accurately access the trends of change across the Earth's surface, to measure ecosystem status and health, understand spatial patterns of biodiversity and for developing land management policy. Over the conterminous United States sixteen classes of land cover were modeled at a 30m cell size with 1 acre minimum mapping unit. According to the 2016 database from NLCD land cover classification in US the percent of barren land was 1.02%, crop land 15.90% and grass land herbaceous was 13.89% which tend to be changing every year, contemporarily it seems database supporting large area land system science monitoring are comparatively rare and change detection monitoring is not regularly carried out (Homer et al., 2020). From the point of view of land system science land cover and its change is a medium for the interaction of nature and its society (Meyfroidt et al., 2018). Homer et al. (2020) argued that demand for longer temporal duration with frequent, accurate and consistent land cover classification along with analogous information about change continues to further drive

the development of land system science monitoring. Any change in the land use and land cover type alters the biophysical surface characteristics and consequently results to major penalties that includes intensification of climate change, land degradation, and changes to biological diversity and ecosystem services (Foley et al., 2011; Pielke, 2005; Rindfuss et al., 2004; Zeleke & Hurni, 2001). Variation in vegetation due to increased aerodynamics roughness over the highly exposed and flattened terrain may produce considerable difference in snow accumulation (Rasmus, 2005). This makes it necessary to understand how different land cover affects snow metamorphism characteristic. Hence in this research, I have tried to study snow metamorphism with physical based model and application of hyperspectral imaging on three different land types such as cropland, grassland and barren surface respectively.

CHAPTER 3

METHODOLOGY

In this chapter, the research methods followed in this study are described. It provides information about the study site, data source, field data collection techniques and the research design. A list of instruments used for data collection and their specifications were included. An energy flux model considered to calculate snow metamorphism and the statistical methods used to analyze the results was discussed. The processing of snow reflectance information from hyperspectral imaging spectroradiometer was also presented. Finally the problems associated with field data collection had been addressed here briefly. Below a flow chat is given in Figure 1 that briefly represents the Study Design of this research:
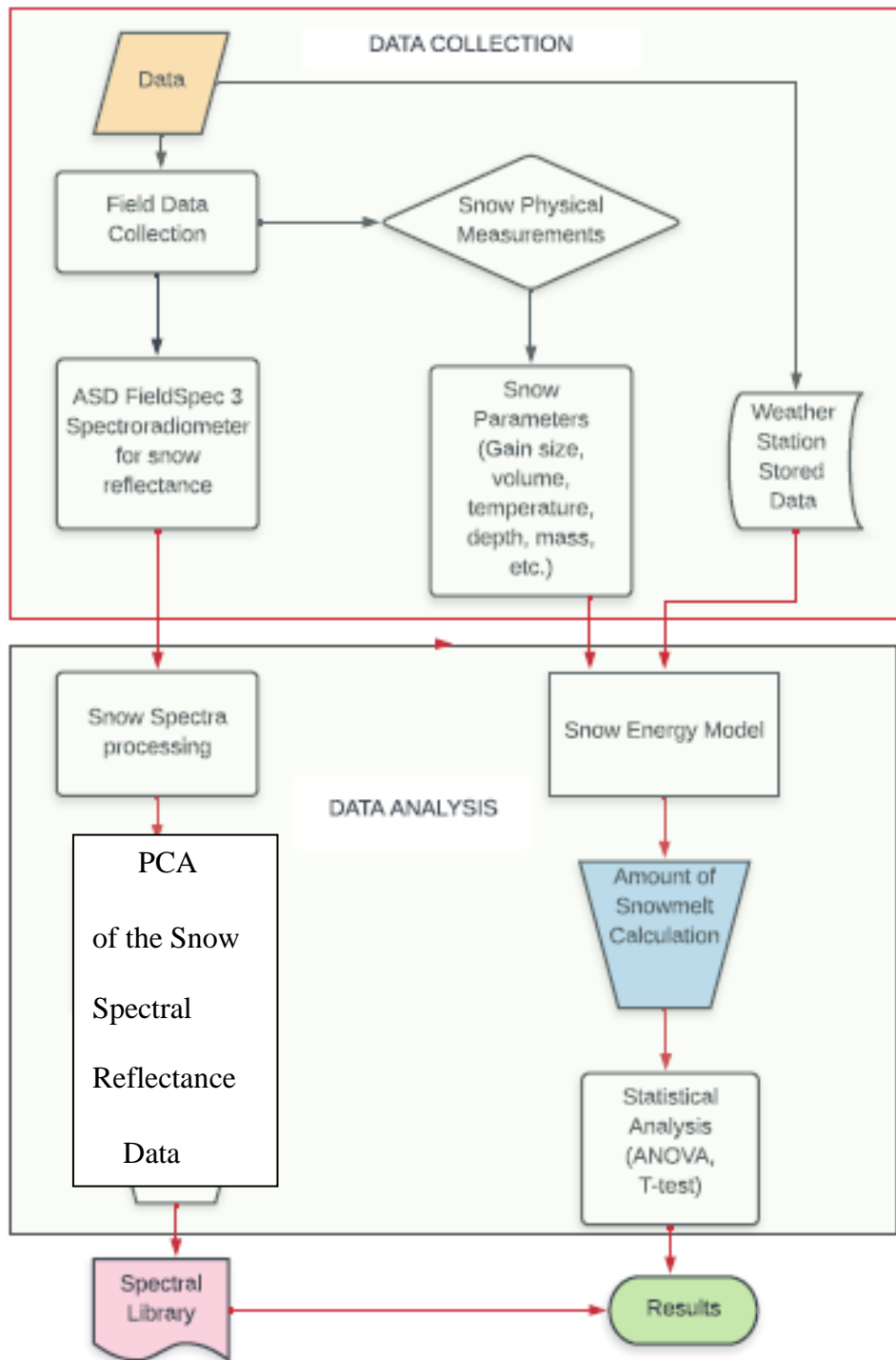
Figure 1. A Flow Chart of Study Design

<u>3.1. Description of the Study Area</u>

The study area described below in terms of its locality and history of the place; topography; its drainage systems; regional climate and land cover types namely - cropland, grassland and barren surface respectively, as follows:

<u>Location of study site</u>. The geographic location of the study site is 42.518009 N, - 92.471163 E, situated at a distance of approximately 100 - 200 meters north-west from the University of Northern Iowa Dome and Wellness/ Recreation Center in Cedar Falls. Software package ArcGIS (version 10.7.1) was used to create a map of the study area and data visualization (Figure 2).
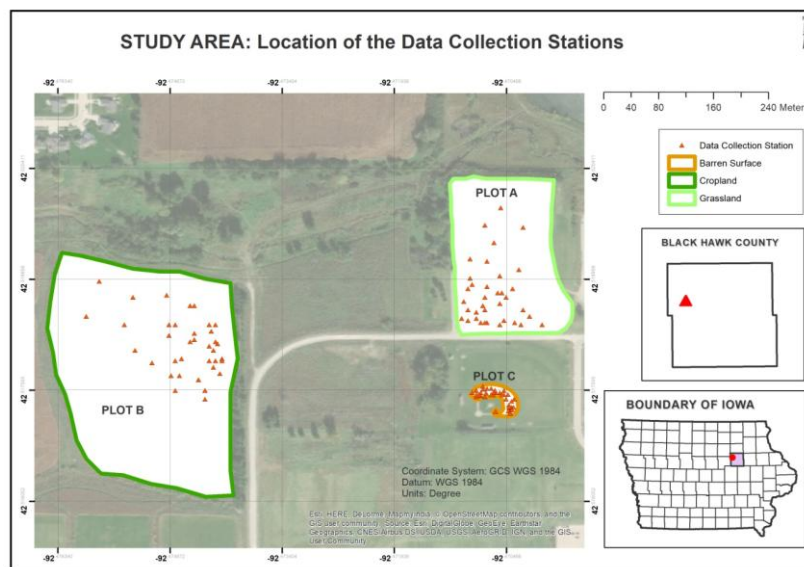
Figure 2. Map of the Study Area along with different Stations Location in cropland, grassland and barren surface

(a)   (b)

(c)

Figure 3. Pictures of land types considered for studying Snow Metamorphism: a. Cropland (Plot B); b. Barren surface (Plot C); c. Grassland (Plot A).

With 150 years of intensive land use the city of Cedar Falls constitutes to exist as a fairly large urban area in the agricultural landscape of Iowa that continues to hold significant biodiversity and a complex natural environment (RDG Planning and Applied Ecology Services, 2012). A relatively small portion of area in Cedar Falls was selected for this research that consists of three different types of land classes for data collection on

snow metamorphism which was separated into three different plots. PLOT – A grassland size 100x100 m^2, PLOT – B cropland size 100x100 m^2 containing corn residues in it and PLOT – C barren surface inside the soccer playground having sand confined in a 25x25 m^2 area were considered for this study respectively. All three plots are tree less open ground receiving good amount of snowfall and sunlight which represents an ideal condition for conducting this research. The average elevations of the plots are 268 m above sea level and the ground is undulating terrain with slight ups and downs in some places.

Land cover types of Black Hawk County. According to Steckly (2006), Black Hawk County land use consisted of 72 percent of cropland; 20 percent of urban land; 5 percent used as recreational land; 2 percent was woodland and only 1 percent containing pasture land. Black Hawk County also contains a considerable portion of sandy areas formed due to wind or water depositions (Norman & Karen, 1987).

Topography and drainage systems. The topography of Black Hawk County consists of long, gentle slopes with open views; less rounded ridges and wide almost level valleys that have unclear ends and well-formed low gradient drainage systems. Here the main drainage system is the Cedar River; the Wapsipinicon River and Black Hawk Creek (Steckly, 2006). The surface of Black Hawk County is mainly made up of the valleys of the Cedar and the Wapsipinicon rivers and their wide spread tributaries such as Beaver creek, Dry Run, Black Hawk, Miller, Big and Rock Creeks in the west, and Elk, Indian and Spring creeks in the east of Cedar, and the Crane creek of Wapsipinicon along with the Iowan plains lie between both side of these valleys (Arey, 1906).

      <u>Climatic conditions of Iowa</u>. Iowa is situated in the Midwestern USA and its climate chiefly governed by the latitude, continental location, and large scale circulation patterns and from the presences of Great Lakes (Andresen et al., 2012). Generally, Iowa experiences four climatic seasons: during the month of January, when it was cold and dry, the winter temperature fluctuates in an average between 14 °F (-10 °C) in its north western part to 20 °F (about – 6 °C) towards its southeast respectively. Compared to the other northern and eastern states in the USA winter snowfalls in Iowa are lighter and the snow cover remains there during the entire winter months. Though heavy snowfalls was recorded in Iowa in the late autumn and early springs but the summers in Iowa appears to be much warmer and humid with its July temperature varies between mid-80 °F (30 °C) to 100 °F (38°C) very rarely when it becomes extremely hot. Beside this, precipitation in Iowa changes according to seasonal basis with an average annual rainfall varies between 26 inches (660 mm) in the northwest to as high as greater than 38 inches (965 mm) in the south eastern part of Iowa (Salisbury & Honey, 2019). Also it was observed in past, atypical conditions like rapid snowmelt and rainfall in Iowa caused severe flooding during the winter time of the year 2007-2008. Therefore, it is important to study Iowa's climate because its variability encompasses the effects of climate change phenomenon that makes it useful for land surface energy flux model.

Below figure represents daily snow conditions like snowfall rate, snow depth and precipitation rate from December till March in Cedar Falls Area, 2019 as follows:
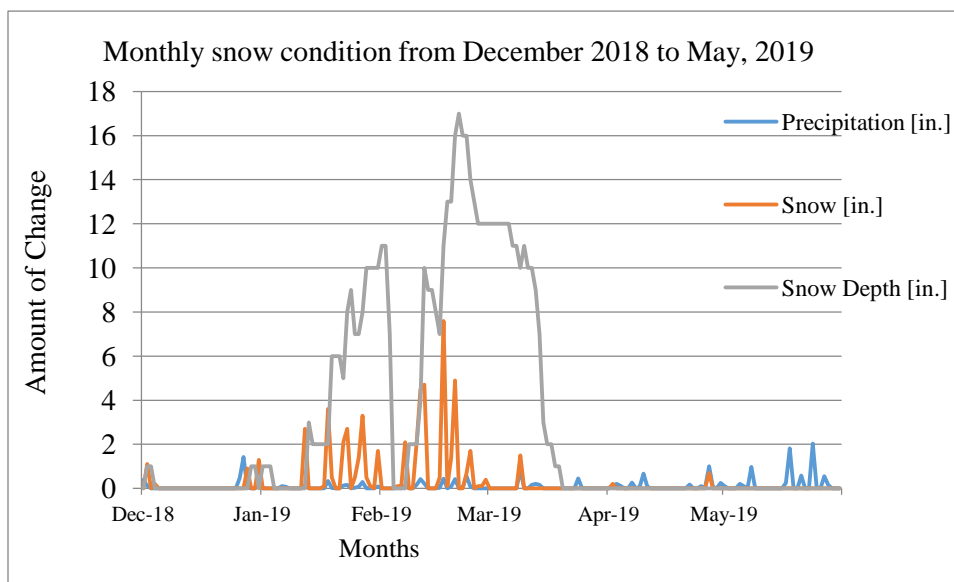
Figure 4. Snow condition before, during and after the study period at Cedar Falls in 2019.

Source: U.S. Department of Commerce National Oceanic & Atmospheric Administration National Environmental Satellite, Data, and Information Service. Station at Waterloo Municipal Airport, IA US WBAN: 72548094910 (KALO)

The above graph in Figure 4 shows how the snow conditions changed from December to March in the year 2019. Small amount of snowfall occurred in the month of December however from the middle of January periodic snowfall occurred till the first week of March after which only traces of snowfall was observed. An increase in snow depth was observed during the end of January till March. Small amount of precipitation

in the form of rainfall was also observed in the beginning of January that lasts for the entire study period and beyond in different dates particularly.

3.2. Research Design

This study relied on quantitative methods, using both numerical data that were analyzed using mathematical based models and observations of specific conditions of snow metamorphism like how, when and why certain changes were taking place.

Primary data source and its collection techniques. Field data collection is both time consuming and tedious in nature but it is very important for ground truthing of remote sensing information. Ground truth enables calibration of the remote sensing data; it helps in the interpretation and analysis of the sensed information. Therefore, the primary source of data for this study was based on ground observations using various tools and techniques to quantify snow metamorphism across cropland, grassland and barren surface respectively. *In-situ* measurement of the physical properties of snowpack such as: snow grain size, snow surface temperature, snow depth and snowpack volume were recorded from each field stations on particular field days and during specific time, i.e., from 11:30 AM to 3:30 PM respectively. An approximate distance of 16.4 feet was maintained between each sampling stations over three different plots on particular field day to avoid disturbance to its surrounding environment. 5 to 3 random stations were selected per land type on each field day to collect data on snow physical properties. The duration of data collection from each field stations was about 5 to 10 minutes. Dates for field data collection were as follows: 01/19/2019, 01/26/2019, 02/01/2019, 02/08/2019, 02/11/2019, 02/15/2019, 02/15/2019, 02/16/2019, 02/18/2019, 02/22/2019, 02/27/19 and

03/05/19. An interval of 1 to 6 days in between each consecutive field day was implemented to allow the snow to change its physical conditions. A total of 114 stations were selected for sampling *in-situ* data of snowpack physical properties across three different land classes. Days having cloud cover <40 % were considered for field data collection. Cloud cover or sky cover is defined as the fraction of the sky covered with clouds reported in tenths (U.S.A.) (Pizarro, 1967). Beside this, unfavorable weather conditions like strong windy conditions and precipitation were avoided since it could transform the snow cover considerably (Pomeroy & Jones, 1996) that causes difficulty in acquiring snow reflectance with spectroradiometer (ASD Inc., 2010). As *in-situ* measurements of physical properties of snow vary in space and time, observation practices and land cover type (Lemke et al., 2007) and in open environment wind causes evolution of snow cover (Pomeroy & Brun, 2001). Therefore, the measurements of snow physical properties were found to be varying with space and time in this study. Below is the full list of instruments used for field data collection of snow physical properties in three different land classes is given in Table 1:

Table 1

Field Instruments used for Data Collection

Sl. No.	Instruments	Usage
1	ASD FieldSpec 3 Spectrodariometer (spectral range 350-2500 nm)	For obtaining spectral signature of the snow reflectance.
2	Fluke 561 IR Thermometer	For measuring snow temperature in degree Celsius.
3	Canon Camera DS 126311 (18mm-136mm lens)	To take the photographs of the object under study.
4	HOBOware Pyranometer (model: 19HS)	To record the solar long wave and short wave radiance
5	Hanna Instrument (Soil temperature probe)	To take the soil surface temperature measurement in degree Celsius.
6	Garmin *E*trex *GPS* unit	For recording the location of the sample spot in the field.
7	HACH pocket pro pH meter	To measure snow pH.
8	Gridded mesh cards (.5mm, 1 mm and 2 mm)	To observe the snow grain size difference
9	Ruler or scale	To take the snow depth measurement from the ground.
10	Portable weighing scale	To take the mass measurement of the snow in gram

Sl. No.	Instruments	Usage
11	Graduated measuring cylinder (1000ml)	Used for measuring snow volume in field in cubic millilitres.
12	Magnifying Glass (4.5x high power spot lens)	Used for observing the size of snow grains.
13	Sampling tubes	Used for snow sampling.

Table 2 shows an exhaust list of physical parameters with their measuring units recorded from the field stations during the study is given below:

Table 2

List of Parameters with their Symbols and Units of Measurement

Sl. No	Parameters with symbols	Unites
1	Snow depth (S_D)	Inches (in)
2	Snow volume (S_V)	Cubic Millilitre (ml^3)
3	Snow density (S_ρ)	Gram/ml
4	Snow grain size	Millimetre (mm)
5	Snow pH	No unit
6	Snow surface temperature (SST)	Degree Celsius (°C)
7	Solar radiation (R_s)	W m^{-2}
8	Soil Temperature (S_T)	Degree Celsius (°C)
9	Snow reflectance (R_λ)	Nanometres (nm)

Field data for this study was collected during particular dates in the month of January, February till March, 5 of the year 2019 when the ground was covered with snow. The procedure for measurement of the physical properties of snow across cropland, grassland and barren surface and their importance in this study was briefly discussed below:

Snow Surface Temperature (SST) measurement. Temperature difference in the snow pack relates to the differences in air temperature, thermal conductivity of snow, terrain, vegetation, elevation and the amount of sunlight (Leppanen et al., 2015). And it acts as a lower boundary condition of the atmosphere over snow-covered surfaces (King et al., 2008). During different field days snow surface temperature was measured and recorded with a Fluke 561 IR Thermometer because the infrared thermometer posses the capacity to determine the snow surface temperature by measuring the amount of infrared energy radiated back from the targeted surfaces. An average of three measurements of the snow surface temperature in Degree Celsius from three different spots per station was recorded from each land type on different field days respectively.

Snow depth measurement. Depth of snow changes considerably with snow accumulation and it is closely related to climate variability; so it is an important physical parameter to understand land surface energy balance (Essery, 2003; Zhong et al., 2018). However, there is a wide range of modern gadgets available in the market to measure snow depth but for this research snow depth at specific point in space and time considered as the vertical distance from the ground surface to the snowpack surface measured with a basic ruler as shown in the Figure 5 below. An average of three snow

depth measurements in centimeters at the same spot from each field stations on individual field day along different land types was recorded respectively.

Figure 5. Instruments used for measuring physical properties of Snowpack: Common Ruler; Garmin Etrex GPS Unit; Weighing Scale; Fluke 561 IR Thermometer; Graduated Measuring Cylinder (1000ml); Container; Gridded Mesh Cards, Record Book; Pencil.

Snow density measurement. Snow density is defined as the relation between snowpack to its water content. Density of snow increases with time and varies according to snow crystal size, shape and the degree of riming (Judson & Doesken, 2000). Reason for the increase in snow density was due to the influence of environmental variables such as - temperature, snow depth, wind, and heat flux (Sturm & Holmgren, 1995). And factors like heat transfer in snowpack were influenced by snow density since snow

thermal diffusivity depends on it (Kay, 2006). It was an important parameter for snow surface energy model so at each station in the study area during a particular time, snow density (ρ_{snow}) from the vertical profile of snow was calculated using the generic formula of density measurement:

$$D = M/V \ (g/ml).......(1)$$

Where, D is the density of snow; M is mass of snow in grams and V is the volume of snow in milliliters. [Note: Conversion 1 g/ml = 1000 kg/m^3]

For measuring the volume of snowpack at different stations a graduated 1000 ml synthetic built transparent measuring cylinder was used to collect snow in field stations. Later the collected snow in the measuring cylinder was weighted on spot with a digital weighing balance to get the mass content of the snowpack which was eventually used to calculate the density of snow per kg per meter cube area as shown in the Figure 6 below. An average of three snow volume measurements per station was considered to make the readings more accurate for this study. Variation in snow density according to different snow types prepared by Seibert et al. (2015) as showed in below Table 3 was used for classifying snow types accordingly in this research.

Table 3

Snow Density Measurement according to different Snow Types

Snow Type	Density (kg m^{-3})
New snow (immediately after falling in calm conditions and at very low temperature)	10–30
New snow (immediately after falling in calm conditions)	50–70
Wet new snow	100–200
Settled snow	200–300
Depth hoar	200–300
Wind packed snow	350–400
Wet snow	350–500
Firn	500–830
Glacier ice	850–917

Based on DeWalle and Rango, 2008; Fierz et al., 2009; Maidment, 1992; Singh and Singh, 2001.

Note. Reprinted from the Snow and Ice in Hydrosphere by Seibert, J., Jenicek, M., Huss, M., and Tracy Ewen, T. (2015), Snow and Ice-Related Hazards, Risks, and Disasters, 102.

Figure 6. Photograph of the method used to measure Density of Snowpack at each field stations.

Snow grain size measurement. Snow grain size was an informational parameter used to analyze snowpack development or metamorphism, and every new weather event amplifies the microstructure of seasonal snow cover (Colbeck, 1982; Greene, 2007). Snow metamorphism meant to be the driver of different snow grain particles shape (Fierz et al., 2009). And the rate of snow grain growth exponentially proportionate to the snow temperature (Jordan, 1991). In this study, the snow grains size at individual station on different field days were measured with gridded cards made-up of hard waterproof papers consisting different grid sizes of 0.5 mm, 1.0 mm and 2.0 mm and a magnifying lens respectively. It was the most convenient way to measure snow grains under natural environmental condition as mentioned by Nolin and Dozier (2000) in their research. After

the snow grain size were measured from each stations on individual field days the snow particles later classified based on grain size according to Singh et al. (2010) category such as: fine (<0.5 mm); medium (<1.0 mm) and coarse (1.0–2.0mm) categories respectively.

Snow spectral reflectance collection. Another important parameter used in this study was the spectral reflectance of snow from three different classes of land types under natural condition. Snow reflectance depends strongly upon snow grain size and the spectral variations in the ice absorption coefficient (Hyvärinen & Lammasniemi, 1987). Here snow reflectance was taken from a randomly selected spot at a height of 2cm in cropland, grassland and barren surface on different field days with an ASD FieldSpec 3 spectroradiometer instrument respectively. For the purpose of the instrument calibration a standard white reference panel was used. The white reference panel or white reference standard is a material with 95 – 99% reflectance across the entire spectrum (ASD Inc., 2010). After all the data were collected the snow spectral reflectance was computed by taking the ratio between the snow radiance to the reference radiance i.e., the white reference panel meant to be almost-Lambertian (Pirazzini et al., 2015) in MS Excel format. The formula used for obtaining the spectral reflectance of snow from spectroradiometer data were as follows: $R(\lambda)$ = (Er) the target spectra divided by (Ei) spectrum of calibrated panel per unit wavelength (Clark, 1999).

$R(\lambda) = E_r(\lambda)/E_i(\lambda)$ [i.e., energy reflected from object at wavelength λ ÷ energy incidence on calibrated panel at wavelength λ].

   <u>Principals of ASD FieldSpec 3 Spectoradiometer</u>. A spectroradiometer is a special kind of spectrometer built for measuring radiant energy (radiance and irradiance). The ASD FieldSpec 3 spectoradiometer is particularly designed for remote sensing of the field environment to obtain visible near-infrared (VNIR) and short-wave infrared (SWIR) spectra (ASD Inc., 2010). This instrument covers a wavelength range of 350 – 2500nm with 3 nm spectral resolutions in its VIR and NIR region, and 10-12 nm spectral resolution at SWIR region (Singh et al., 2010). It is a non-imaging, portable, faster, real-time and more accurate device (Pishva, 2011). The reflective property of any object collected by the spectroradiometer were at high resolution and of more precision particularly meant for identification, quantification, and detection of objects (Hueni & Tuohy, 2006). Table given below showed the ASD FieldSpec 3 spectroradiometer wavelength configuration at VNIR, SWIR 1 and SWIR 2 respectively.

Table 4

FieldSpec 3 Spectroradiometer Wavelength Configuration

Wavelength Name	Wavelength Range
VNIR-SWIR1-SWIR2	350 - 2500 nm
VNIR only	350 - 1050 nm
VNIR-SWIR1	350 - 1800 nm
SWIR1 only	1000 - 1800 nm
SWIR1-SWIR2	1000 - 2500 nm
SWIR2 only	1800 - 2500 nm
VNIR & SWIR2	350 - 1050 nm and 1800 - 2500 nm

Source: ASD Inc. (2010). Solar illumination factors. ASD Document Rev. J, p. 3
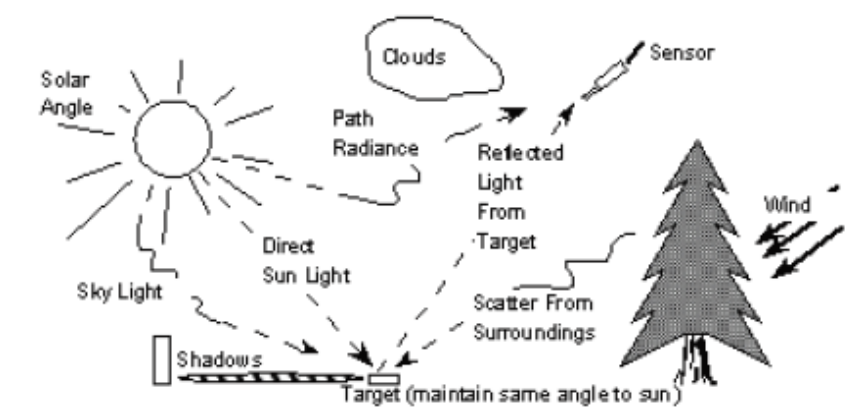
Figure 7. Schematic Diagram: Factors to consider under solar illumination to measure

Reflectance of an object with ASD Field Spec 3 Spectroradiometer

Source: ASD Inc. (2010). Solar illumination factors. ASD Document Rev. J, p. 68

Meteorological data collection. Secondary data used to estimate amounts of snowmelt at each field station were the principal meteorological data such as: wind speed, air temperature, atmospheric pressure and temperature at dew point retrieved from a Davis Vantage PRO2 instrument fixed on the roof top of Latham Hall at the University of Northern Iowa during different field days from 11:30 AM to 3:30 PM respectively. A list of meteorological parameters along with their units of measurement used in this research was given in Table 5.

Table 5

List of Meteorological Parameters with their Units of Measurement

Sl. No.	Parameters	Units
1	Wind speed	Mph
2	Air temperature	Degree Celsius (°C) or Fahrenheit (°F)
3	Relative Humidity	RH
4	Long wave and short wave solar radiation	Wm^{-2}
5	Precipitation	Mm

Sun is Earth's primary source of power, energy from the sun as solar irradiance drives Earth's climate, temperature, weather, atmospheric chemistry, ocean cycles, energy balance, etc. (Merzdorf, 2020). Incoming solar radiation - global or total insolation is the amount of solar energy reaching the earth's surface proved to have many important

applications (Pizarro, 1967). And both radiative and turbulent heat flux transfers were the vital process for snow surface energy exchange (Cline, 1997). Therefore, for estimating the net surface energy flux in snowpack and the amount of snowmelt at each station on different field days in three different land classes at specific time the components of radiative and turbulent heat flux transfer were computed and used in the energy flux model in this study.

Turbulent heat flux in snow energy flux model provides information about loss or gain of heat in the snow pack. Both sensible and latent heat gets transferred between surface and atmosphere by the turbulent process. The sensible heat flux involves a convective flow of heat, whereas, the latent heat flux is an equivalent heat exchange due to phase change i.e., evaporation, sublimation and refreezing (Pomeroy & Brun, 2001). Because the components of sensible and latent heat fluxes in a snow model were based on meteorological data at a given layer in the atmosphere and at the snow surface (Martin & Lejeune, 1998). Alteration in internal energy of snowpack was due to the sensible heat and latent heat storage, therefore, these were computed with various parameters taken into consideration as reported by Datt et al. (2008).

The steps to create baseline information from the data collected in the field stations and from the meteorological instrument installed at University of Northern Iowa were as follows:

Data processing steps. *In-situ* data of snow physical condition such as: snow grain size, snow surface temperature, snow depth and snowpack volume measurements collected from each field stations in different field days at specific time across three

different land classes were systematically compiled in the Microsoft Excel format. Meteorological data such as: wind speed, air temperature, atmospheric pressure and temperature at dew point retrieved from Davis Vantage PRO2 weather device on particular field days at specific time from 11:30 am till 15:30 pm were averaged individually per day and used in this research. Then both the *in-situ* data and the meteorological data were utilized for computing the net surface energy flux in the snowpack per station to estimate the amounts of snowmelt in cropland, grassland and barren surface individually respectively. Beside this, snow reflectance were taken across cropland, grassland and barren surface separately from a random sampled spot with the help of high resolution spectroradiometer (ASD FieldSpec 3) during different field days to use for detecting snow metamorphism from ground based hyperspectral imaging. Detail description about estimating the amounts of snowmelt at different stations and statistical analysis of the results had been illustrated below:

3.3. Estimation of Amounts of Snow on different Land Types and Statistical Analysis

In this step, collected data was processed using energy flux model given by Datt et al. (2008) and Cline et al. (1998) and analyzed for hypothesis testing described below:

Calculation of net snow surface energy flux. Past studies had described the process of snow melting (e.g., US Army Corps of Engineers, 1998; Gray & Male, 1981; Dingman, 1994; You, 2004) primarily driven by energy exchanges at the snow–air interface (Tarboton et al., 1995). This lead to the development of models of snowmelt process differently with variable complexities ranging from simple methods using only temperature measurements to complex multilayer models (Marks et al., 1999), such as

the US Army Cold Regions Research and Engineering Laboratory Model (Zanotti et al., 2004). Perhaps snow pack energy balance determines the distribution of temperature in the snow cover (Rasmus, 2005). In this research, I have used temperature based energy flux model to estimate amount of snowmelt across cropland, grassland and barren surface respectively. To understand the process of snow energy flux model a schematic diagram was produced below in the Figure 8 to illustrate the process visually.
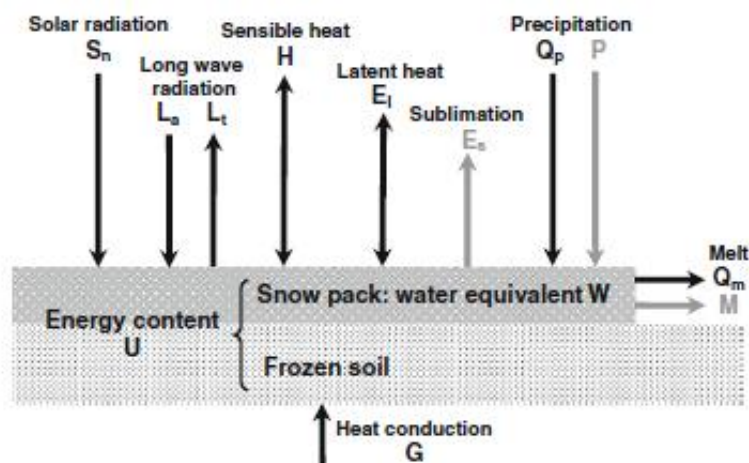
Figure 8. Schematic representation of energy and mass fluxes involved in snowpack accumulation and Melt: Sn net solar radiation, La atmospheric long-wave radiation, Lt terrestrial long-wave radiation, H sensible heat exchange, El latent heat of vaporization or condensation, Qp heat brought with precipitation, Qm amount of heat removed by snowmelt, G ground heat flux, U snowpack's internal energy, P precipitation, Es sublimation, and M snowmelt intensity

Source: Zeinivand & de Smedt (2009). Prediction of snowmelt floods with a distributed hydrological model using a physical snow mass and energy balance approach. Natural Hazards, p. 454

To understand the physical condition of snow, i.e., either melting or cooling (re-freezing) it was necessary to observe the net energy flux in snowpack. Cold content in snowpack increases when the net energy flux becomes negative which reduce the snow layer temperature, similarly cold content in snow layer decreases when the net energy flux in snowpack becomes positive. Beyond a specified threshold melt water from snow does not outflow (Sensoy et al., 2006). So here net energy flux over the snow surface across cropland, grassland and barren surface was calculated individually on particular day at specific time to know the amounts of snowmelt by using an energy flux model given by Datt et al. (2008) and Cline et al. (1998) as follows:

$$\Delta Q = S_{in} + S_{out} + L_{in} + L_{out} + H\text{se} + H_{la} + H_{R,} \quad W/m^2 \,.........(2)$$

Where, ΔQ = net energy flux at the surface, Sin and $Sout$ = incoming and outgoing shortwave fluxes, and Lin and Lout = incoming and outgoing long-wave radiation. Hse = the sensible heat flux and Hla = latent heat flux. As the heat flux due to snowfall and rainfall on snow $H_{R,}$ and ground heat flux were negligible according to Datt et al. (2008), so these parameters were not considered in this study.

The short-wave radiation incident from the sun towards the snow surface was taken as positive, whereas, the short-wave radiation going out from the snow surface was considered as negative. Furthermore, since the surface of the snow also exchanges long-wave energy flux with the surrounding atmosphere, therefore, the long-wave energy flux *(Lout)* emitted by the surface was computed by using Stephan's formula as follows:

$$\text{Lout} = \varepsilon s\sigma T_a^{\,4}, \; W/m^2 \,............(3)$$

Where, εs = emissivity of the snow surface close to unity, σ = Stefan Boltzmann constant and T_s = snow surface temperature in *Kelvin*. The remaining incoming long-wave radiation (*L*in) was estimated by using the parameterizations given by Prata (1996) model that calculate the emissivity of atmosphere in terms of perceptible water. In this study, the emissivity of snow surface considered was 0.97 as constant according to Datt et al. (2008). The formula used for clear-sky downward long-wave radiation was as follows:

$$L\text{in} = \varepsilon s \sigma T_s^{\,4}, \; W/m^2 ....(4)$$

Then after calculating the *Lin* and *Lout* from the above equation the final net long-wave radiation *(R$_{nl}$)* were estimated by subtracting *Lout* from *Lin*.

Finally, for estimating the net solar radiation *(R$_{ns}$)* resulting from the balanced equation between incoming and reflected radiation the following equation given by Malvern (2014) and Raes (2009) was used as follows:

$$R_{ns} = (1 - \alpha) \, R_s.......(5)$$

Where, R_{ns} = net solar or short-wave radiation (W/m^2 per day); R_s = incoming solar or short-wave radiation (W/m^2 per day), α = snow albedo. It was important to note that although fresh snow albedos were higher than those of aged snow (Coakley, 2003), but since *in-situ* measurement of snow albedo was not recorded on particular field days hence an intermediate value between fresh and aged snow albedo considered here was .66 as used by Cline (1997) and Briegleb et al. (1986) in their study. Before plug-in the value

of Rs in the above equation (5) the solar radiation was estimated from the formula that uses the sunshine hours given by Trajkovic et al. (2011) as follows:

$$R_s = (0.25 + 0.5 \, n/N) \, R_a........(6)$$

Where, n = actual duration of sunshine (hour); N = maximum possible duration of sunshine (hour); and R_a = extraterrestrial radiation (MJ m-2 d-1) at top of atmosphere. Moreover, for computing clear-sky solar radiation and maximum duration of sunshine hours when $n=N$ the formula given by Raes (2009) was used as follows:

$$N = (24/\pi) \, \omega_s...........(7)$$

Where, N = daylight hours and ω_s = sunset hours in radians (ϕ). And ω_s was calculated from the following equations:

$$\omega_s = arcos \, [-tan \, (\phi). \, tan \, (\delta)]...........(8)$$

$$Radians \, (\phi) = (\pi/180) \, [decimal \, degree]............(9)$$

$$\delta = 0.409 \, sin \, (2\pi/365) \, J \, -1.39.............(10)$$

Where, J = number of the day in the year between day 1 (1 January) and 365 or 366 days (31 December). The value of latitude (ϕ) was considered positive since the study area was situated in the northern hemisphere otherwise, for the southern hemisphere it would be negative.

Extraterrestrtal radiation/theoretical radiation/potential insolation *(Ra)* is defined as the amount of solar energy that reaches the outer atmosphere and there exists a suitable relation between solar radiation and extraterrestrial radiation (Pizarro, 1967). So the Extraterrestrial radiation *(R_a)* for each day of the year and for current latitude was calculated from the solar constant, the solar declination and the time of the year in the units MJ m^{-2}. min^{-1} as follows:

$$R_a = [(24\ (60))/\pi]\ G_{sc}\ d_r\ [\omega_s\ sin\ (\phi)\ sin\ (\delta) + cos\ (\phi)\ cos\ (\delta)\ sin\ (\omega_s).........(11)$$

The inverse relative distance between Earth-Sun was denoted by d_r which was calculated with the following equation:

$$d_r = 1 + 0.033cos\ [(2\pi/365)\ J]..........(12)$$

Where, R_a = extraterrestrial radiation [MJ m^{-1} day $^{-1}$]; G_{sc} solar constant = 0.0820 MJ m^{-2} min; d_r = inverse relative distance between Earth-Sun (Equation 12); ω_s = sunset hours angle; ϕ = latitude in radian (Equation 9); δ = solar decline (Equation 10).

Eventually, the net radiation was computed by adding the net surface shortwave radiation *(R_{ns})* and long-wave radiation (R_{nl}) as given by Krishna et al. (2014) as follows:

$$R_n = R_{ns} + R_{nl} = (R_s\downarrow - R_s\uparrow) + (R_l\downarrow - R_l\uparrow)\ W/m^2...........(13)$$

Where, $R_s\downarrow$ = downward short-wave radiation; $R_s\uparrow$ = upward short-wave radiation; $R_l\downarrow$ = downward long-wave radiation; $R_l\uparrow$ = upward long-wave radiation

Due to the radiative properties of snow the area covered with snow is generally associated with stable atmospheric boundary layer and the measurement of sensible and latent heat fluxes in stable stratification were rare phenomenon (Martin & Lejeune, 1998). Therefore, turbulent energy components were calculated by using bulk transfer approach given by Deardroff (1968) as follows:

$$H\text{se} = \rho a Ca Ch Ua(Ta - Ts)........(14)$$

$$H\text{la} = (\rho a L Mv/PaMa)Ce Ua \{Ei(Ta) - Ei(Ts)........(15)$$

Where, ρa = air density, Ca = specific heat of air, Ua = wind velocity above the snow surface, L = latent heat of sublimation, Pa = atmospheric pressure, Mv = molecular weight of water vapour, Ma = molecular weight of dry air, Ei = saturation vapour pressure, Ta = air temperature, Ts = snow surface temperature, Ch = heat transfer coefficient and Ce = humidity transfer coefficient. Moreover, the bulk transfer equations were adjusted for stability of the atmosphere using the Richardson number (Ri) for neutral, stable and unstable atmospheric conditions (Hong et al., 1992).

Components such as actual vapor pressure (e_a) and atmospheric emissivity (ϵ_a) was estimated by using the dew point temperature (T_{dew}) and vapor pressure values using the following equation given by Krishna et al. (2014):

$$e_a = e^0 (T_{dew}) = a exp [bT_{dew} / (T_{dew} + 237.3)]..........(16)$$

$$\epsilon_a = a [e_a/ (T_a + 273.15)]^b...................(17)$$

Where, e_a estimating unit was in hPa, its value was 6.11 and b was 17.27 used as constants. T_a = air temperature, a and b for equation (17) = calibration constants having the value of a = 1.24 and b = 0.143; σ = Stefan-Boltzmann constant (5.67 x 10^{-8} W/m^2-K^4).

Estimation of amounts of snowmelt. Finally, to estimate the amount of snowmelt at each sampling stations the following equation mentioned by Datt et al, (2008) was used as follows:

$$dm = \Delta Q \ (\rho s c \Delta t + Lf \rho s)..........(18)$$

Where, dm = amount of snowmelt, ρs = density of snow, Lf = latent heat of fusion, c = specific heat of snow and Δt = the temperature required to bring snow at 0°C. The snow surface energy flux ΔQ was assumed to get absorbed in the top layer of snow of thickness dm.

Statistical analysis methods used. TIBCO Spotfire S-Plus (version 8.2) analytical software was used to perform parametric statistical analysis across three land classes under study. One-way analysis of Variance (ANOVA) was considered to check the statistical significance of the mean values of the amounts of snowmelt over the land classes. It is an analysis of variance test very useful for hypothesis testing that compares the mean of two or more independent groups in order to determine the statistical evidence that the associated means of the data in use are significant. Box and whisker plot on the estimated amounts of snowmelt results from three different land classes was drawn to display the distribution of data based on five number summary i.e., minimum, first

quartile (Q1), median, third quartile (Q3), and maximum. Box and whisker plot is an explanatory data analysis technique where the graph displays the distribution, shape, central value and the viability of the grouped data. Also, two-sample T-test analysis was done on the computed amounts of snowmelt for each day at different stations across the three land classes to check the statistical significance. The two-sample T-test basically considers the sampled group data and boils it down to t-value then it compares the sample mean(s) to the null hypothesis and incorporates both the sample size and viability in the data respectively.

The prevalent method for spectral analysis was based on relating the morphological features of the spectra i.e., the position and depth of an absorption band with the amount of a certain material responsible for the absorption (Clark & Roush, 1984; Green & Craig, 1985). Principal Component Analysis (PCA) was a widely used technique for spectral compression and reduction that decompose a spectral data set into linear combinations of several main spectral components (Tsai et al., 2007; Rinnen et al., 2015). It was considered to be the most recognized technique for dimension reduction while preserving the information in hyperspectral data (Fountanas, 2004). Therefore, Principal Component Analysis (PCA) in IBM SPSS statistical software was carried out on ASD FieldSpec 3 spectroradiometer snow reflectance data set collected during particular field days at specific time. PCA reduces the continuum between the data obtained and identifies the components that are useful for detecting snow metamorphism in snowpack, and yields information about possible indicative band(s) that correspond to

certain snow conditions after the influence of the original bands on the data variability was given by the factor loadingsrs (Hueni & Tuohy, 2006; Thenkabail et al., 2004).

<div align="center">3.4. Snow Spectral Library</div>

Hyperspectral sensors typically measure the brightness of an object in its hundreds of narrow contiguous wavelength bands (Fountanas, 2004). For correct interpretation of information from remote sensing data, quickly recognizing the matching unknown features and improve remote sensing classification (Herold et al., 2004; Dudley et al., 2015). Finally, spectral libraries were developed from a collection of snow surface reflectance spectra with hyperspectral imaging spectroradiometer that determines characteristics of snow metamorphism on different days at specific time across cropland, grassland and barren surface respectively.

CHAPTER 4

RESULTS

Being a fine-grained material snow possesses high specific area which remains active thermodynamically due to close to melting point (Colbeck, 1982). Any change in snow properties are driven by the energy, mass and momentum exchange in the surface and bottom boundaries of snow pack. Due to the fact that ground frost are impenetrable; therefore, surface boundary conditions are important for the change (Rasmus, 2005). The prevalent meteorological conditions such as air temperature, relative humidity, precipitation, wind velocity, short-wave and long-wave radiation are the driving forces for changes in snow properties respectively. In this chapter, the results from snow energy flux model are presented. The characteristics of snow metamorphism had been compared and discussed between cropland, grassland and barren surface and its detection with hyperspectral imaging technology was shown. Results of statistical analysis of the estimated amounts of snowmelt among cropland, grassland and barren surface was presented and hyperspectral bands representing snow metamorphism characteristic were determined. Spectral libraries from snow reflectance spectra on different dates along different land types are presented according to different snow grain size respectively. Also, importance of each component used to estimate amounts of snowmelt in different land classes is discussed. Lastly, additional characteristics of snow metamorphism observed during the study period are presented.

4.1. Snow Density

The fundamental physical property of snow is its density influenced by the meteorological condition during snowfall and snow pack process (Kay, 2006). And forecasting snowfall could be improved by detail analysis of snow density (Roebber et al., 2003; Stoelinga et al., 2005). Change in temperature induces alteration in snow density. At constant temperature the snow pack becomes compact, new snow deposition increases the pressure on former snow results in an increase in the snow density and grain metamorphism (Leppanen et al., 2015). Grains shape in seasonal snow changes (Colbeck, 1982) very rapidly and the size of grains gets increased with the age and depth of the snowpack (Leppanen et al., 2015). Variation in snow grain size was observed during the study in different field days and across different land class. For understanding the relationship between snow grain size with density and categorizing the snow types according to snow density, individual tables were prepared with snow grain size, snow density and snow types for the three different land class viz., cropland, grassland and barren surface (Table 6, Table 7 and Table 8) with reference to Seibert et al. (2015) above Table 3.

Table 6

Classification of Snow Types for Cropland according to Snow Grain Size and Snow

Density

Cropland			
Dates	Snow Grain Size (mm)	Snow pack Density (kg/m^3)	Snow Types
01/19/19	.5	226	Settled Snow/Depth Hoar
01/26/19	.5	238	Settled Snow/Depth Hoar
02/01/19	1	397	Wind packed Snow/ Wet Snow
02/08/19	.5	317	Settled Snow/Depth Hoar
02/11/19	.5	271	Settled Snow/Depth Hoar
02/15/19	.5	309	Settled Snow/Depth Hoar
02/16/19	1	322	Settled Snow/Depth Hoar
02/18/19	.5	234	Settled Snow/Depth Hoar
02/22/19	2	308	Settled Snow/Depth Hoar
02/27/19	2	417	Wind packed Snow/ Wet Snow
03/05/19	2	401	Wind packed Snow/ Wet Snow

Snow density range from about 200 kg/m^3 to 300 kg/m^3 was identified as settled or depth hoar snow type and snow range from about 350 kg/m^3 to 500 kg/m^3 was identified as wind packed snow or wet snow in this study

Table7

Classification of Snow Types for Grassland according to Snow Grain Size and Snow Density

Grassland			
Dates	Snow Grain Size (mm)	Snow pack Density (kg/m^3)	Snow Types
01/19/19	.5	225	Settled Snow/Depth Hoar
01/26/19	.5	238	Settled Snow/Depth Hoar
02/01/19	.5	418	Wind packed Snow/ Wet Snow
02/08/19	1	319	Settled Snow/Depth Hoar
02/11/19	2	264	Settled Snow/Depth Hoar
02/15/19	1	306	Settled Snow/Depth Hoar
02/16/19	1	309	Settled Snow/Depth Hoar
02/18/19	.5	261	Settled Snow/Depth Hoar
02/22/19	2	330	Settled Snow/Depth Hoar
02/27/19	2	444	Wind packed Snow/ Wet Snow
03/05/19	2	428	Wind packed Snow/ Wet Snow

From the above two tables 6 and 7 it was found that in the case of cropland and grassland 73 percent of the snow belonged to the category of settled snow or depth hoar type having snow grain size .5mm to 1mm, whereas, 27 percent of the snow belonged to wind packed or wet snow category with snow grain size of 2mm approx. respectively.

Table 8

Classification of Snow types for Barren Surface according to Snow Grain Size and Snow

Density

Barren Surface			
Dates	Snow Grain Size (mm)	Snow pack Density (kg/m^3)	Snow Types
01/19/19	.5	227	Settled Snow/Depth Hoar
01/26/19	1	238	Settled Snow/Depth Hoar
02/01/19	1	357	Wind packed Snow/ Wet Snow
02/08/19	2	365	Wind packed Snow/ Wet Snow
02/11/19	2	241	Settled Snow/Depth Hoar
02/15/19	.5	282	Settled Snow/Depth Hoar
02/16/19	1	286	Settled Snow/Depth Hoar
02/18/19	1	316	Settled Snow/Depth Hoar
02/22/19	2	452	Wind packed Snow/ Wet Snow
02/27/19	2	427	Wind packed Snow/ Wet Snow
03/05/19	2	464	Wind packed Snow/ Wet Snow

For barren surface a small change was observed, it was found that 45 percent of the snow belonged to settled or depth hoar type having snow grain size ranging from .5mm to 1mm and 55 percent falls under the wind packed or wet snow category having snow grain size of 2mm approx. respectively.

Table 9.

Summary Statistics Chart of Snow Density across grassland, cropland and barren surface

	Cropland	**Grassland**	**Barren Surface**
Min	226	225	227
1st Quartile	254.50	262.50	284.00
Mean	312.72	322.00	341.36
Median	309.00	309.00	341.00
3rd Quartile	359.50	374.00	396.00
Max	417	444	464
Variance	4695.21	5938.40	6641.25
Std Dev.	68.52	77.06	81.49
SE Mean	20.66	23.23	24.57
Sum	3440	3542	3755

The summary statistics in Table 9 shows the minimum snow density in barren surface was 227 kg/m^3, cropland was 226 kg/m^3 and grassland was 225 kg/m^3, and the maximum snow density in barren surface was 464 kg/m^3, grassland was 444 kg/m^3 and cropland was 474 kg/m^3 respectively. The mean snow density in barren surface was 341.36 kg/m^3, grassland was 322.00 kg/m^3 and cropland was 312.72 kg/m^3. The snow density standard deviation for barren surface was 81.49, grassland was 77.06 and cropland was 68.52, and their Standard Error was 20.66, 23.23 and 24.57 respectively.

Snow Density Vs Snow Grain size

- 0.5mm
- 1mm
- 2mm

Snow Density (kg/m³)

Grassland: 285.41, 311.31, 366.4
Cropland: 266.06, 359.96, 375.11
Barren surface: 324.29, 299, 364.40

Land Types
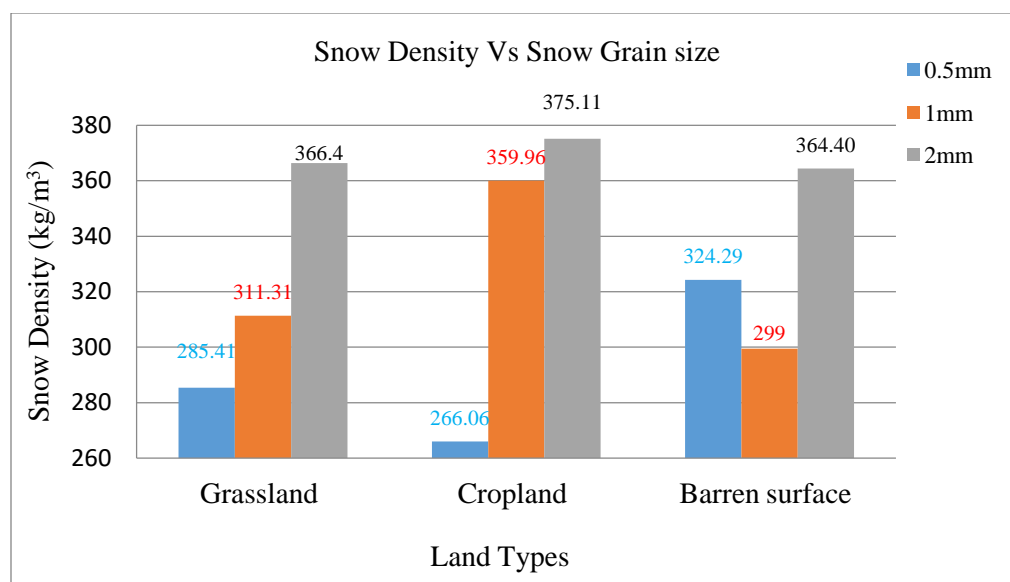
Figure 9. Variation in average snow density with snow grain size between grassland, cropland and barren surface

Average density of snow and snow hardness depends upon the underlying vegetative pattern (Rasmus, 2005). After averaging the snow density according to grain size for cropland, grassland and barren surfaces the above graph in Figure 9 shows snow density in different land types increased with the increase in snow grain size, except in barren surface where the average snow density decreased when the snow grain size increased to 1mm. The result reflects at .5mm snow grain size the snow density in barren surface was 324.29 kg/m³, the snow density in grassland was 285.41 kg/m³ and cropland was 266.06 kg/m³ respectively. When the grain size increased to 1mm the snow density in cropland increased to 359. 95 kg/m³, snow density in grassland increased to 311.31 kg/m³ but snow density in barren surface decreased to 299 kg/m³. Lastly when the snow

grain size increased to 2mm the density of snow in cropland increased to 375.11 kg/m^3, grassland snow density increased to 366.4 kg/m^3 and snow density in barren surface increased to 364.40 kg/m^3 respectively.
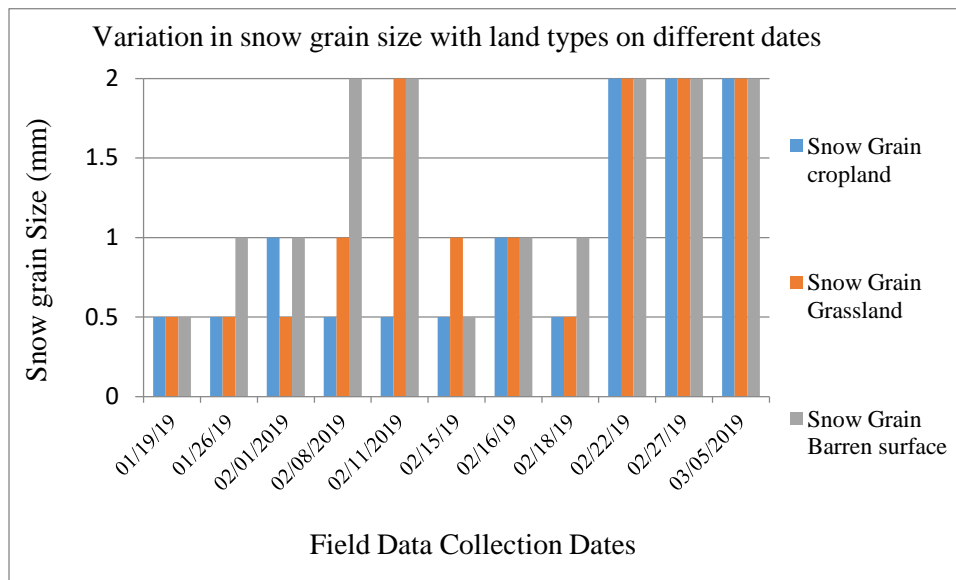
Figure 10. Difference in snow grain size across cropland, grassland and barren surface on different field days

Figure 10 shows snow grain size varies along different terrain features and with different field days. At the beginning and in the end of the field days the snow grain size appeared to lie at 0.5mm and 2mm for grassland, cropland and barren surface respectively. However, on other field days the snow grain size had changed implicitly for

different land types respectively. This indicates variation in snow metamorphism and redistribution of snow crystals by wind.

4.2. Radiation Fluxes

Components of radiation are influenced differently by the surface heterogeneity and with the presences, type and diurnal distribution of clouds that makes the net radiation over the surface change both spatially as well as temporally (Krishna et al., 2014). The radiation flux enhanced the melting of snow at different sites on different days. Below is a graph showing net radiations changes with time and space during different field days in this study.
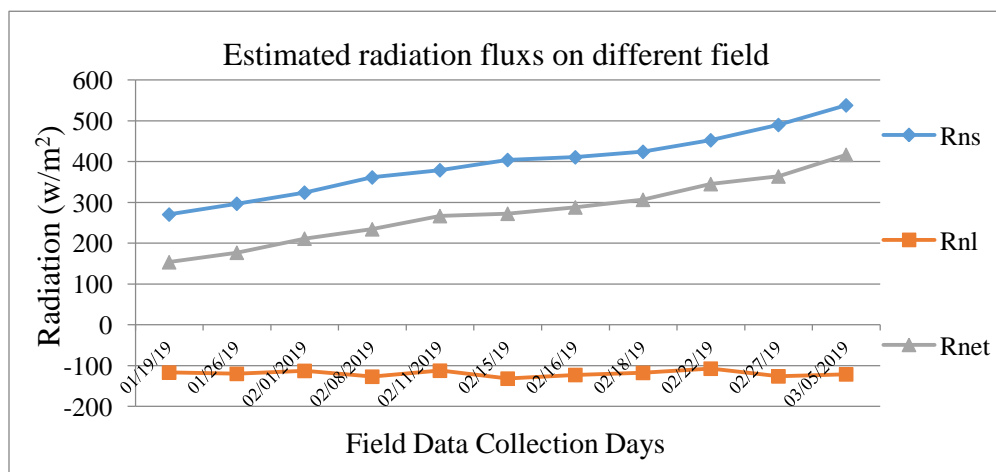
Figure 11. Graph showing estimated net radiation over snow surface (Rnet), net long-wave radiation (Rnl) and net shortwave radiation (Rns) per field day during specific time in the study area.

Figure 11 shows changes in the estimated net radiation flux over the snow surface, net shortwave radiation flux and net long-wave radiation flux on different field days respectively. The shortwave radiation flux from sun and the net radiation flux showed a positive inclination with the progress in field days, whereas, the net long-wave radiation flux appeared to be negative and steady with small fluctuations in this study. The estimated minimum net long-wave radiation flux was found -131.8 W/m^2 in the first day of the data collection, whereas, the maximum net long-wave radiation flux was found -107.383 W/m^2 on the last field day. On the other hand the minimum shortwave radiation flux was estimated 270.525 W/m^2 on date 01/19/19 that increased to maximum 538.200 W/m^2 on date 09/05/19. Also, the minimum net radiation flux was estimated 153.61 W/m^2 on date 01/19/19 that increased to 416.97 W/m^2 when it was 5th March the last day of the field data collection for this research. Beside this, the above graph also reflects the estimated net long-wave radiation flux leans almost parallel to the shortwave radiation flux. The increase in net radiation rise the internal temperature of the snowpack to melt the snow respectively.
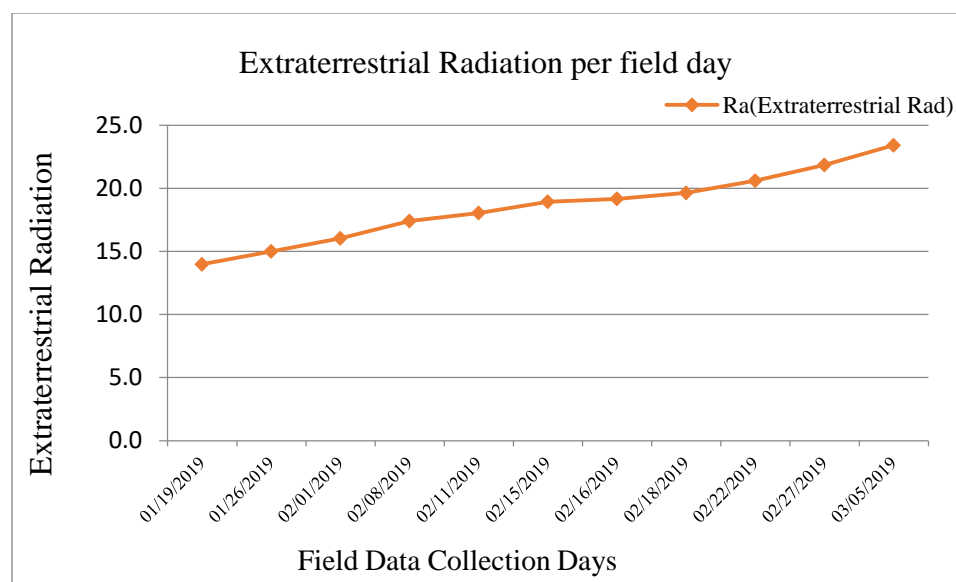
Figure 12. Extraterrestrial Radiation on individual field days at top of atmosphere

The above graph in Figure 12 in this study showed an increase in the extraterrestrial / solar radiation at top of atmosphere with the progress in field days. The minimum value of extraterrestrial radiation was found 14.0 MJ m^{-2} min^{-1} on date 01/19/2019, whereas, the maximum value was 23.4 MJ m^{-2} min^{-1} on date 03/05/2019 and the mean value of the Extraterrestrial radiation was 18.6MJ.m^{-}2.min^{-1} respectively. Extraterrestrial radiation is the intensity of the solar radiation incident horizontally outside the earth's atmosphere that increases with the days depending on the months of the year.

Table10

Summary Statistics of Snow Surface Energy flux (W/m^2) for cropland, grassland and barren surface.

	Cropland (W/m^2)	Grassland (W/m^2)	Barren Surface (W/m^2)
Min	153.69	153.66	153.85
1st Quartile	223.06	222.96	222.77
Mean	276.21	276.11	276.06
Median	272.45	272.47	272.23
3rd Quartile	326.32	326.13	326.12
Max	417.04	417.02	417.11
Variance	6437.10	6431.22	6429.64
Std Dev.	80.23	80.19	80.18
SE Mean	24.19	24.17	24.17
Sum	3038.34	3037.29	3036.67

The above Table 10 shows very minute differences in snow surface energy flux between cropland, grassland and barren surface. The minimum values of snow surface energy flux were 153.69, 153.66 and 153.85 W/m^2 for cropland, grassland and barren surface, whereas, the maximum snow surface energy fluxes were 417.04, 417.02 and 417.11 W/m^2 over the three land types respectively. The standard deviation of snow surface energy fluxes were 80.23, 80.19 and 80.18, and the standard mean error were 24.19, 24.17 and 24.17 for grassland, cropland and barren surface.

4.3. Amounts of Snowmelt Due to Net Radiation Flux in Cropland, Grassland and Barren

Surface during Particular Field Days
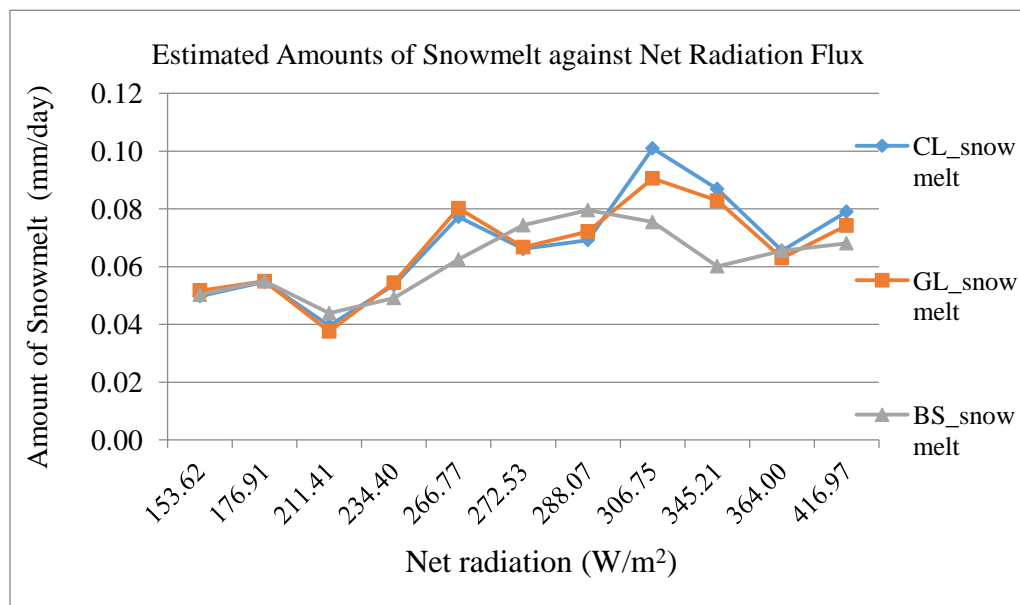
Figure 13. Graph represents amounts of snowmelt due to net radiation flux on different

field days across cropland (CL), grassland (GL) and barren surface (BS)

The above graph (Figure 13) represents changes in the estimated amounts of

snowmelt for cropland, grassland and barren surface with changing in net radiation flux

in the study area during different field days. The amounts of snowmelt in cropland and

grassland appeared almost similar from the beginning which differs a little at the end.

However, the estimated amounts of snowmelt in barren surface showed a different

pattern compared to the other two land types in this study. Increasing-decreasing pattern

in snowmelt in the three different land classes represents a variation in cold content in

snow pack per field day with respect to change in net radiation flux. Overall the amounts of snowmelt in different land class showed a rise with the increase in net radiation flux in this study.

4.4. Amounts of Snowmelt and Turbulent Heat Flux across Grassland, Cropland and Barren Surface

(a)Amounts of snowmelt *Vs* Turbulent Heat Flux in cropland
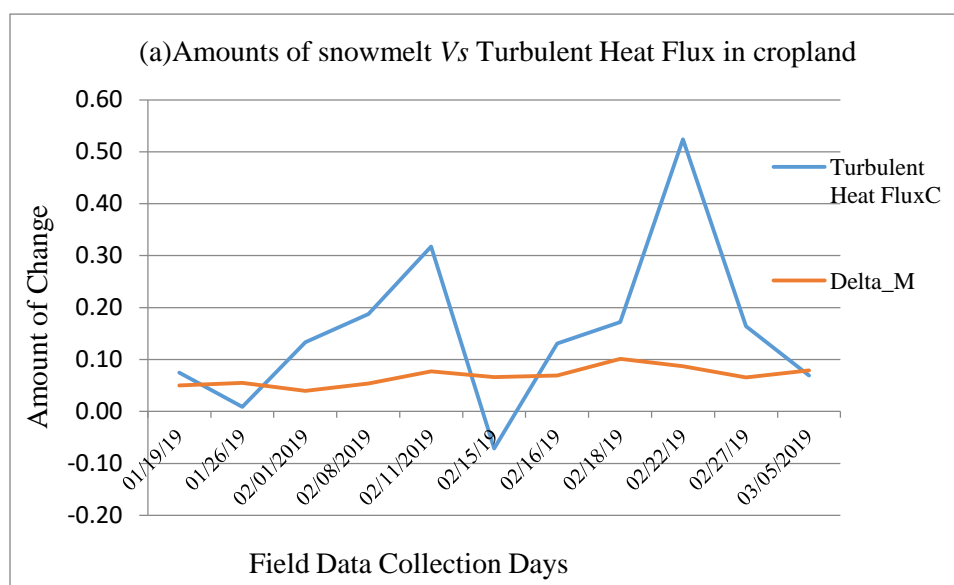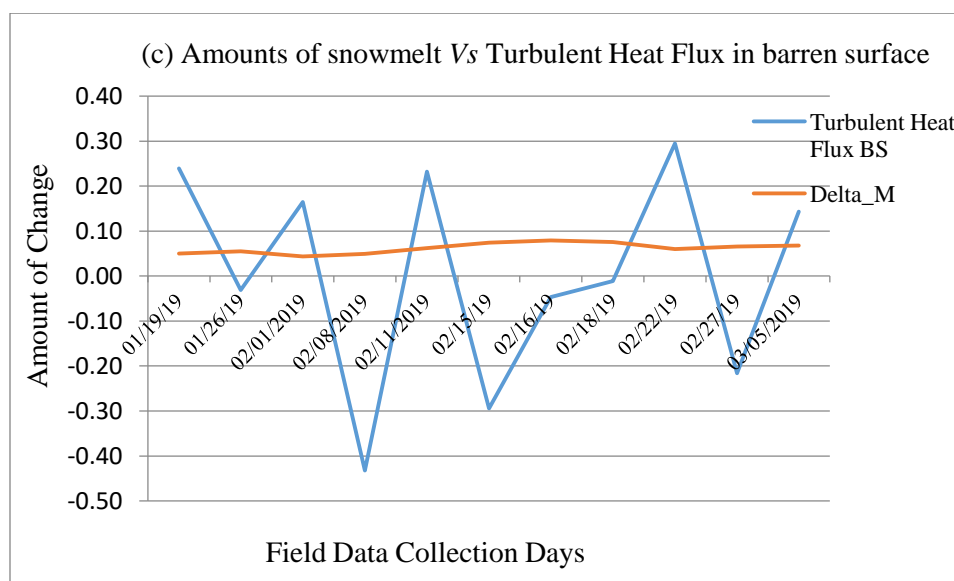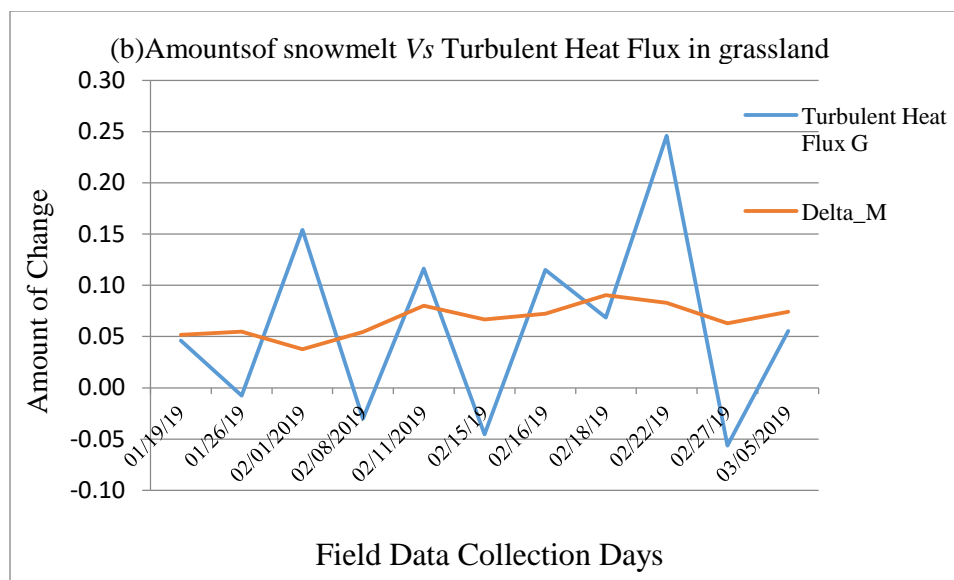
Figure 14. On different dates (a) Graph showing amounts of snowmelt against turbulent heat flux in cropland (C); (b) Graph showing amounts of snowmelt against turbulent heat flux in grassland and (G) (c) Graph showing amounts of snowmelt against turbulent heat flux in barren surface (BS). Delta_M = Snowmelt

From the above graphs (Figure 14) turbulent heat flux was found to fluctuate randomly from positive to negative in grassland, cropland and barren surface during different field days at specific time period. However, the amounts of snowmelt in different land types showed positive and appeared to be almost steady compared to the turbulent heat flux. An increasing-decreasing pattern of turbulent heat flux revel an unstable type of conditions above the snow surface. The positive values of the turbulent fluxes indicates gain of energy by the snowpack, whereas, the negative values indicate a loss of energy from snowpack (Cline, 1997) across different land types in this study.

4.5. Comparison between Total Average Snow Surface Temperature and Average Air Temperature per Field Day in the Study Area

	01/19/ 2019	01/26/ 2019	02/01/ 2019	02/08/ 2019	02/11/ 2019	02/15/ 2019	02/16/ 2019	02/18/ 2019	02/22/ 2019	02/27/ 2019	03/05/ 2019
Ts (F)	9.4	4.7	6.0	6.4	24.2	11.8	20.7	16.8	21.6	12.8	12.9
Ta(F)	12.6	4.3	10.3	4.0	27.7	7.4	23.0	19.7	31.2	12.1	14.5
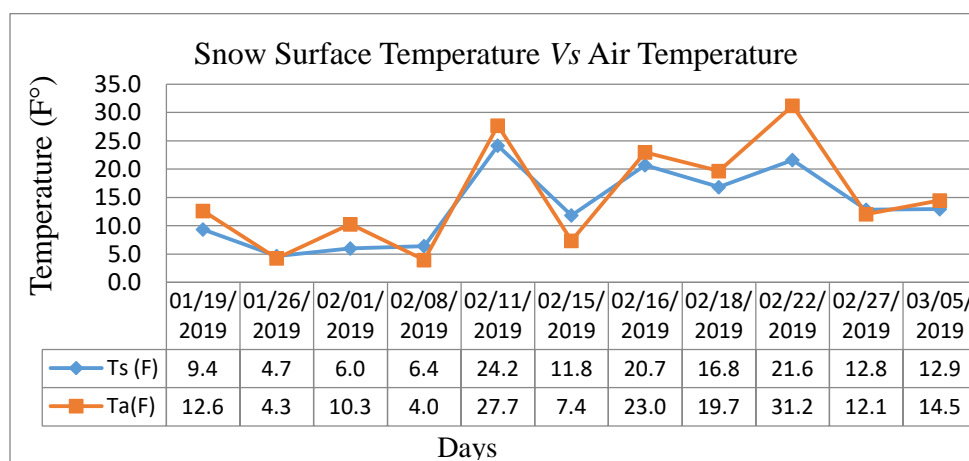
Figure 15. Graph showing comparison between averaged snow surface temperature in total and air temperature during particular field days and at specific time period in the study area Ta = Air Temperature; Ts = Snow surface Temperature.

The above graph (Figure 15) showed an increasing-decreasing pattern for both the snow surface temperature and air temperature on different field days at specific time period in the study area. In this study, the average low and high snow surface temperature was found in the range from 9.4 (F°) to 20.7 (F°) and the average low and high air temperature was found in the range from 4 (F°) to 23 (F°) in the study area respectively. Snow surface temperature is an important factor in the snow energy balance and land-atmosphere interaction that determines energy used to warm or melt a snowpack (Raleigh et al., 2013). The product of air temperature and wind speed used in this study was vital for heat fluxes in snow (Hasebe & Kumekawa, 1995). The mean snow surface temperature was 13.4 (F°) and the mean air temperature was 15.1 (F°) in the study area revealing heat transfer from the surrounding air to the snow for melting. Beside that other components of weather used in this study showed an average wind speed was 6.86 m/s, the mean vapor pressure was estimated 2.28 mb, mean atmospheric pressure was 1028.62 hPa, the estimated mean atmospheric emissivity was .51 hPa and the mean calculated saturated vapor pressure was 3.21 hPa during the field days respectively which also influenced snow metamorphism.

4.6. Comparison between Snow Surface Temperature in Cropland, Grassland and Barren

Surface and Average Air Temperature on Different Field Days in the Study Area
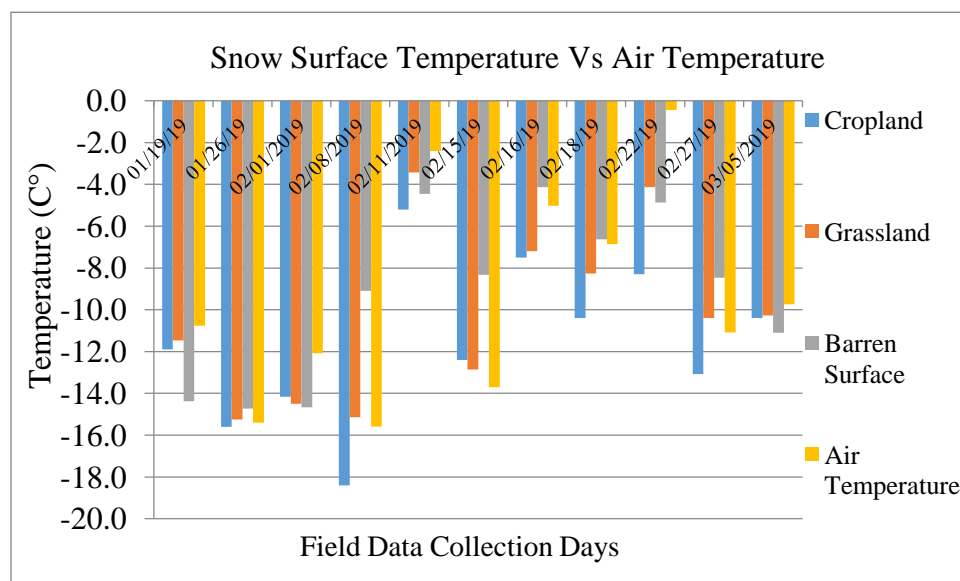
Figure 16. Comparison between average snow surface temperature over grassland, cropland and barren surface against average air temperature in the study area on different field days

The above graph shows variation in the average snow surface temperature over individual land types with the change in surrounding air temperature on different field days in the study area. The average minimum snow surface temperature over cropland was -18.4 C°; grassland was -15.2 C° and barren surface was -14.7 C°, whereas, the average maximum snow surface temperature observed over cropland was -5.2 C°; grassland was -3.4 C° and barren surface was -4.1 C° respectively. The mean snow

surface temperature in cropland was -11.5 C°; grassland was -10.2 C° and barren surface was -9.1 C°. The variance in the snow surface temperature over three land types were 14.3, 17.2 and 16.5. And their standard deviations were 3.7; 4.1 and 4.0. The average minimum and maximum air temperature was -15.6 C° and - 0.4 C°, mean air temperature was -9.3 C°, its variance was 26.0 and standard deviation was 5.1 in the study area during the field days on particular time period respectively. Comparatively lower snow surface temperature over three land types in different field days than air temperature reveals that cold content in the snow pack was high that allows the snow to condense. It also indicates under natural environment, the condition of the snow differs for grassland, cropland and barren surface during different field days respectively.

4.7. Cumulative Amounts of Snowmelt in cropland, grassland and barren surface during

the study period
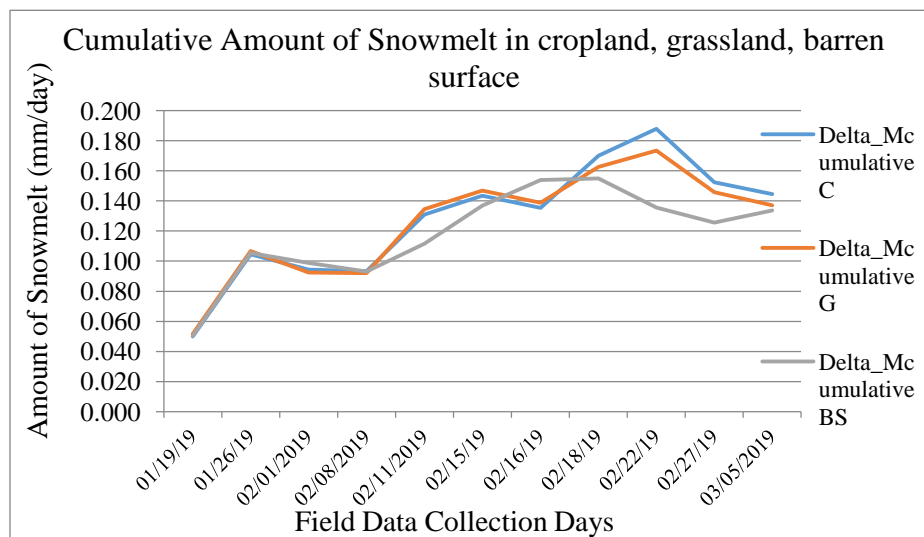
Figure 17. Cumulative amounts of snowmelt in cropland (C), grassland (G) and barren surface (BS) during the study period.

In the above Figure 17, the overall cumulative amount of snowmelt across different land type shows increasing pattern with the progress in field days. It was found that the mean cumulative amounts of snowmelt for grassland was 0.125 mm/day, cropland was 0.127 mm/day and barren surface was 0.118 mm/day, and their variance were .0012, .0015 and .0009 during the study respectively. This study shows that the cumulative amounts of snowmelt varies very little among cropland, grassland and barren surface respectively. Also compared to cropland and grassland cumulative amounts of snow melt in barren surface was little low.

<u>4.8. Statistical Analysis</u>

Table 11

Summary Statistics Chart of Estimated Amounts of Snowmelt (mm/day) in three

different land types

	Cropland (mm/day)	**Grassland (mm/day)**	**Barren Surface (mm/day)**
Min	0.039	0.037	0.043
1st Quartile	0.053	0.053	0.050
Mean	0.066	0.065	0.061
Median	0.066	0.066	0.059
3rd Quartile	0.078	0.077	0.072
Max	0.116	0.093	0.080
Total Samples	38	38	38
Variance	0.0003	0.0002	0.0001
Std Dev.	0.017	0.015	0.011
SE Mean	0.0028	0.0024	0.0018

The above summary statistics chart showed the minimum amounts of snowmelt

on cropland was 0.039 mm/day and the maximum was 0.116 mm/day. For the case of

grassland, the minimum amounts of snowmelt were 0.037 mm/day and maximum

amounts of snowmelt were 0.093 mm/day. In barren surface the minimum amounts of

snowmelt were 0.043 mm/day and maximum amounts of snowmelt were 0.0080 mm/day

during the study period. Mean estimated snowmelt in grassland; cropland and barren

surface were 0.065 mm/day, 0.066 mm/day and 0.061 mm/day respectively. Total samples considered here were 38. The standard deviation for the three different land classes was 0.017, 0.015 and 0.011, and the Standard Error is 0.0028, 0.0024 and 0.0018 respectively.
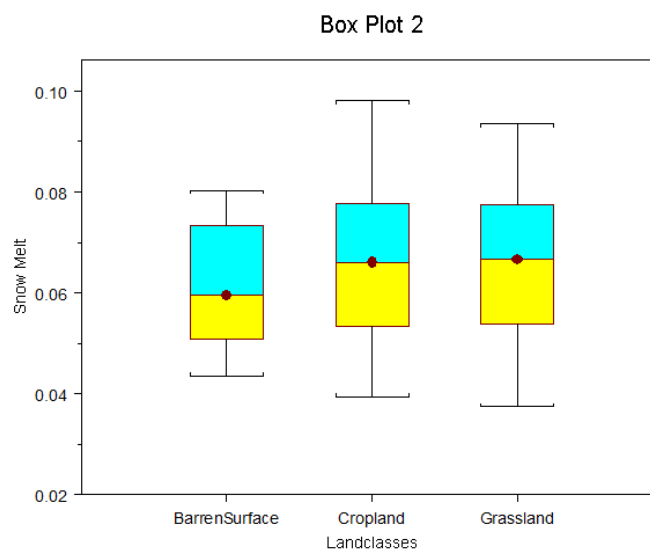
Figure 18. Box and whisker Plot 2 for estimated amounts of snowmelt in cropland, grassland and barren surface.

The box and whisker plot (Figure 18) showed there was no significant difference in the estimated amounts of snowmelt between cropland and grassland. However, the amounts of snowmelt in barren surface were differing little lower than the other two land types. When One-way ANOVA test was performed on the estimated amounts of snowmelt across cropland, grassland and barren surface together it showed a *p-* value of .298 at 2 degree of freedom that seems to be pretty high. Thus, there was no statistically

significant difference in the estimated amounts of snowmelt between cropland, grassland and barren surface. However, the results from t-test on the estimated amounts of snowmelt for grassland, cropland and barren surface were different from the ANOVA test still no statistical significant difference was observed. At 95 percent confident interval the t-test result showed a *p-*value of 0.140 for barren surface and cropland, for grassland and barren surface the *p-*value was 0.190 and a *p-*value of .799 was found for cropland and grassland respectively. This indicates the null hypothesis was accepted for both the statistical test methods over the estimated amounts of snowmelt in three different land classes in this study.

<div align="center">4.9 Snow Condition and Hyperspectral Characteristics</div>

When Principal Component Analysis (PCA) was performed on all the snow reflectance data sets collected with ASD FieldSpec 3 that showed consistent behavior on particular field days. Irrespective of snow grain size, after binding the data sets at 10nm intervals by simple averaging and using only those principal components with eigenvector values >1 within the wavelength range from 350nm to 1039nm respectively. The results from varimax rotation (orthogonal rotation) represented components 1 and 2 were potential for identifying snow metamorphism characteristics in cropland, grassland and barren surface. Component 1 that consists of hyperspectral bands with highest loadings: 1014.5, 1024.5 and 1034.5 nm having the reflectance > 0.1 but < 0.6, whereas, component 2 that consists of hyperspectral bands with highest variance were: 355, 365, 374.5, 384.5 and 394.5 nm having the reflectance > 0.7 but < 0.9. Here varimax factor rotation method was used in order to obtain simple and interpretable factors.

4.10. Determination of Snow Metamorphism with Hyperspectral Imaging Spectra across

Cropland, Grassland and Barren Surface

In this study, only those spectra of the snow reflectance from three different land classes viz., cropland, grassland and barren surface that showed a consistent behavior were used for the detection of snow metamorphism. When spectra of snow reflectance from ASD FieldSpec spectroradiometer were analyzed according to snow grain size measurements and estimated amounts of snowmelt on particular field days for specific time period to check the potentiality of hyperspectral imaging to detect snow metamorphism it showed the following patterns:

(a) Snow Surface Reflectance over grassland
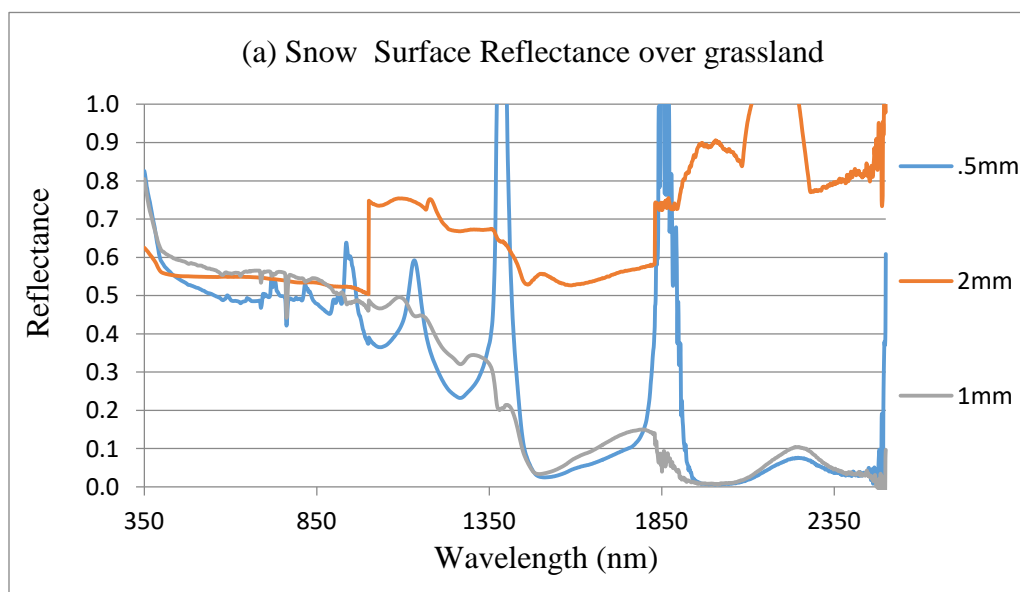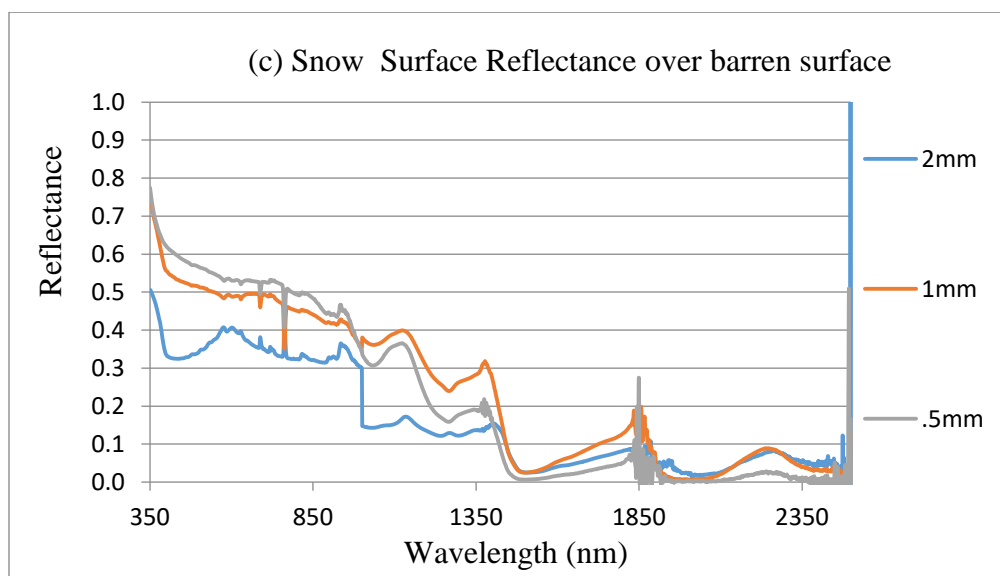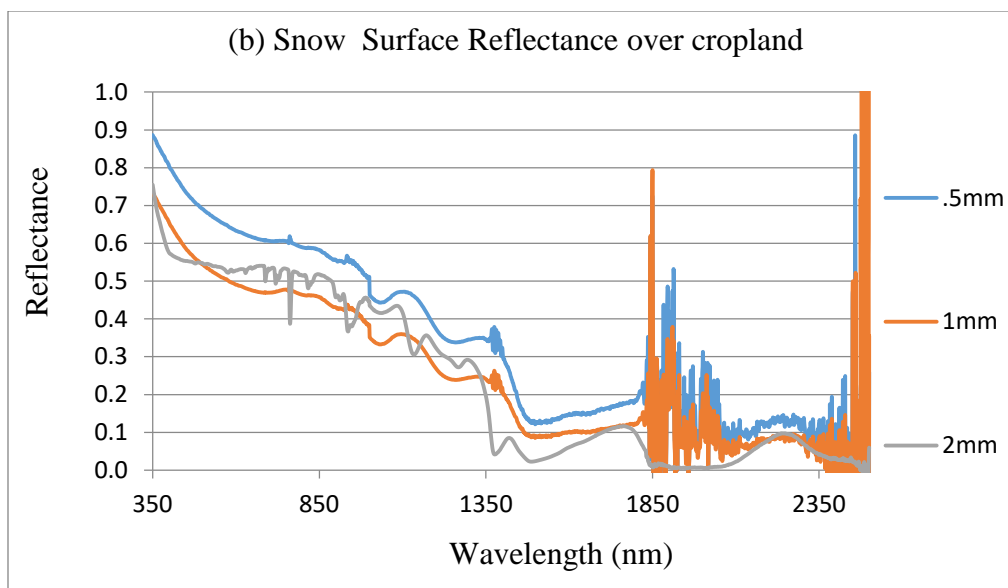
Figure 19. On particular dates at specific time of the day: (a) Shows spectral reflectance of snow metamorphism in grassland; (b) Shows spectral reflectance of snow metamorphism in cropland; and (c) Shows spectral reflectance of snow metamorphism in barren surface.

All of the above spectra in Figure 19 showed high reflectance within the wavelength range from 350nm to 1039nm beyond which the spectra of the snow diminished considerably. Although pure snow particles possessed very high reflectance but lesser than 1, therefore, only the wavelength range between 350nm to 1039nm were found useful for detecting snow metamorphism across grassland, cropland and barren surface in this research. In Figure 19 (a) at .5mm grain size on date 02/01/2019 and 1mm grain size on date 02/15/2019 the spectra of snow reflectance in grassland started at 0.8 that sharply declined at some point between wavelengths 351nm to 400nm after which it appeared to be steady having minute peaks in the wavelength between 401nm to 1039nm. Eventually those spectra showed depression further along the remaining wavelengths, but when the snow grain size increased to 2mm on date 02/11/2019 the reflectance spectra of snow started just above 0.6 decreased a little bit between wavelengths 351nm to 355nm then became steady between wavelengths 356nm till 900nm respectively. After that the spectra suddenly distorted along the remaining wavelengths and showed a sharp rise. In Figure 19 (b) at 0.5mm grain size on date 01/19/2019 the reflectance of snow in cropland started just below 0.9 that gradually declined further along the wavelength between 351nm to 1355nm with minute peaks downswings further along the remaining wavelengths. When the snow grain size increased to 1mm on date 02/01/2019 the snow reflectance spectra started just above 0.7 which showed a depression along wavelength 351nm to 1355nm and later declined further along the remaining wavelengths. At 2mm grain size on date 02/27/2019 the reflectance spectra of snow started at 0.7 declined sharply between wavelengths 351nm to 355nm then inclined upward along wavelength

700nm to 1350nm after that the spectra declined along the remaining wavelengths. In Figure 19 (c) at 0.5mm snow grain size on date 01/26/2019 and 1mm snow grain size on date 02/16/2019 in barren surface the reflectance spectra of the snow started in between 0.8 and 0.7 gets declined along wavelengths 351nm up to 355nm that further showed depression gradually till wavelength 1039nm with minute peaks observed in between the wavelengths. Eventually, after wavelength 1355nm the spectra showed considerable depression along the remaining portion of the wavelengths. But when the snow grain size becomes 2mm on date 03/05/2019 the reflectance spectra of snow started at 0.5 that showed sharp depression between wavelengths 351nm to 355nm and then again inclined upward from wavelength 360nm and later gradually declined further till wavelength 900nm. After that the snow spectra showed a sharp decline in its reflectance, eventually from wavelength 1400nm the reflectance spectra of snow decreased considerably along the remaining portion of the wavelengths respectively.

4.11. Spectral Libraries of Snow Reflectance from Cropland, Grassland and Barren Surface with Different Snow Grain Size

(a) Spectral reflectance at .5 mm. snow grain size reflectance

(b) Spectral reflectance at 1 mm snow grain size
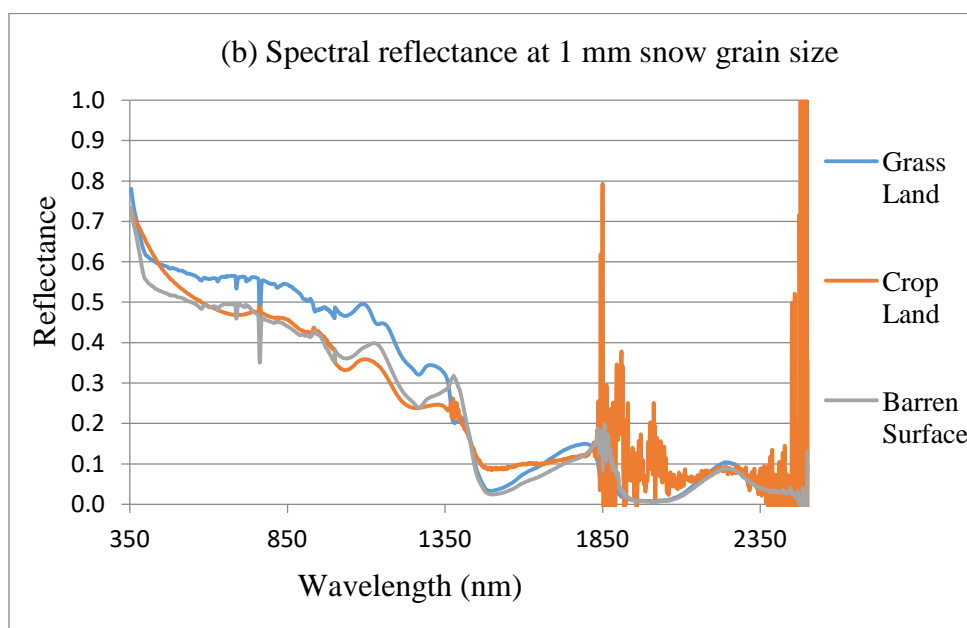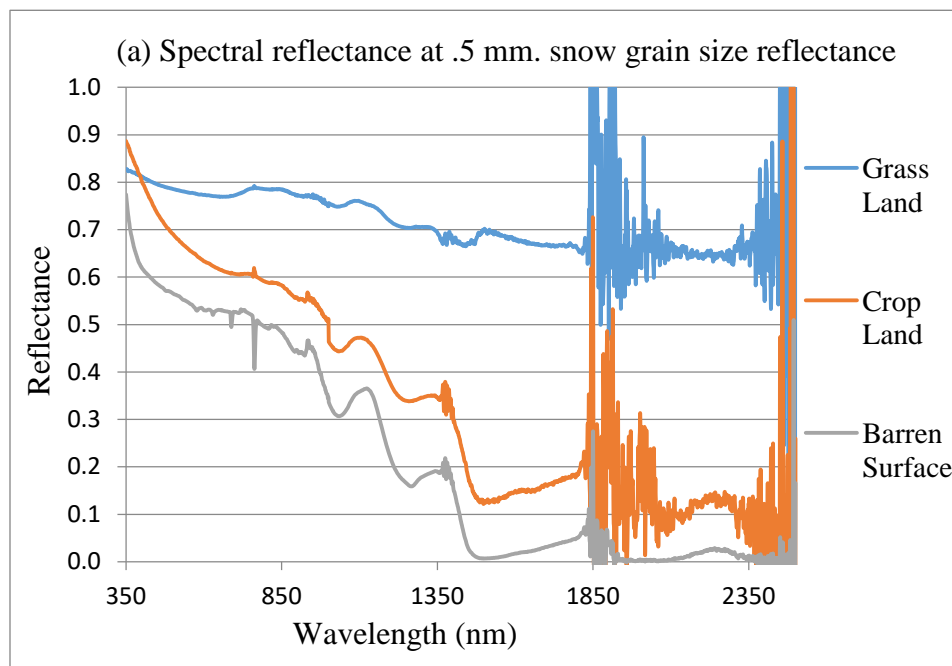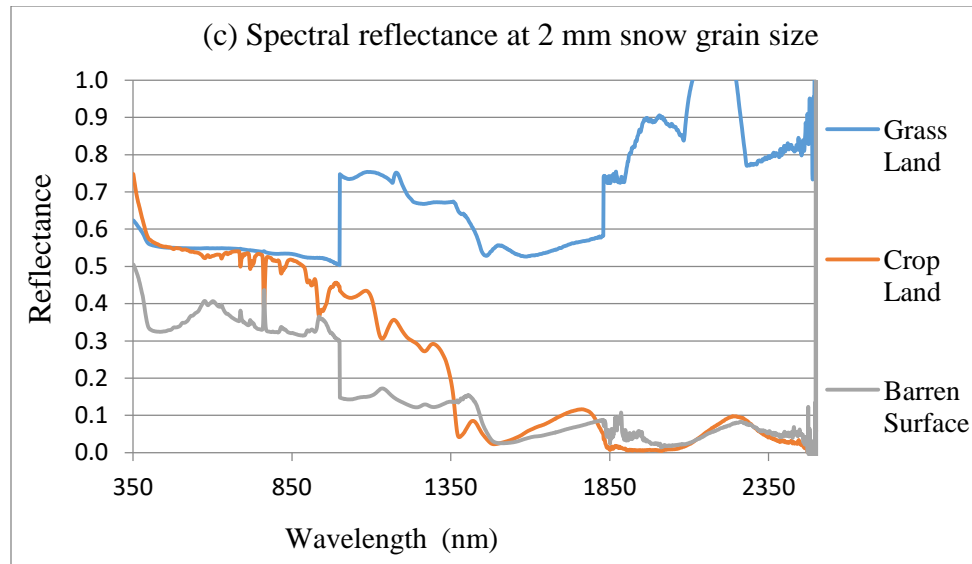
Figure 20. On particular day and specific time period: (a) Spectral reflectance at .5 mm. snow grain size; (b) Spectral reflectance at 1 mm snow grain size; and (c) Spectral reflectance at 2 mm snow grain size, across cropland, grassland and barren surface

Snow reflectivity and snow grain size were negatively correlated which denotes bigger grain size corresponds to lesser snow reflectivity (Zhao et al., 2013). The above spectral libraries in Figure 20 showed when the snow grains increased in size the reflectance over the snow gets diminished for all the three types of land classes under study. Moreover, at different wavelengths and for specific snow grain size the snow spectral reflectance behaved differently for grassland, cropland and barren surface. When the spectra were compared among the three land classes the grassland revel the highest snow reflectance followed by cropland and barren surface which possessed the lowest snow reflectance for different grain size on particular field days during specific time due to difference in melting rate. Moreover, different wavelengths had different absorbing

capacity so even when the snow grain size was found similar the snow reflectance varied for different land classes. In Figure 20 (c) the snow reflectance spectra of grassland showed inconsistent after crossing the wavelength 900nm. This type of spectral behavior was assumed to cause due to malfunction of the ASD FieldSpec 3 spectroradiometer that was used to collect snow reflectance. The following table showed different spectral behavior of snow reflectance with respect to estimated amounts of snowmelt and grain size on particular dates across cropland, grassland and barren surface:

Table 12

Estimated Amounts of Snowmelt on different dates and Grain Size according to different Spectral Reflectance of Snow in use

Date	Land Types	Snow grain size (mm)	Estimated amounts of snowmelt (mm/day)
02/01/2019	Grassland	0.5	0.0375
02/15/2019	Grassland	1	0.0667
02/11/2019	Grassland	2	0.0801
01/19/2019	Cropland	0.5	0.0498
02/01/2019	Cropland	1	0.0395
02/27/2019	Cropland	2	0.0654
01/26/2019	Barren surface	0.5	0.0550
02/16/2019	Barren surface	1	0.0795
03/05/2019	Barren surface	2	0.0680

The above table showed the estimated amounts of snowmelt differed with snow grain size across different land types and along different dates when different snow reflectance spectra were considered. It indicates that there was no perfect relation among snow grain size with estimated amounts of snowmelt in cropland, grassland and barren surface on different dates respectively.

4.12. Additional Characteristics of Snow Metamorphism Observed: "ice-crust" or "melt-

freeze"
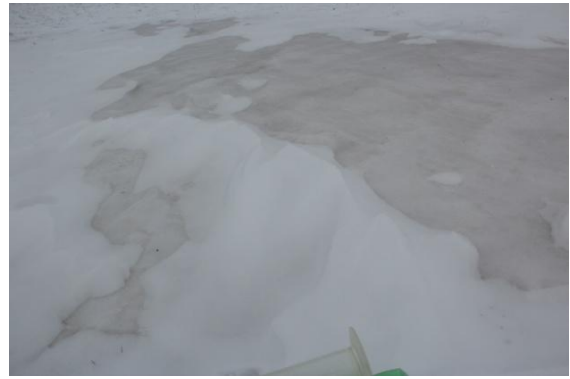
(a)   (b)

(c)

Figure 21. On particular day at specific time period freezing caused (a) Ice cover ground

in cropland; (b) Ice cover over snow in grassland; and (c) Icy ground in barren surface.

In the three different land classes under study, cropland, grassland and barren surface, the above conditions in Figure 21 were observed on date 02/08/2019 during field data collection time. Variation in estimated amounts of snowmelt on different classes of land was observed. The Figure 22 below showed the amount of snowmelt on different land classes on that particular day.
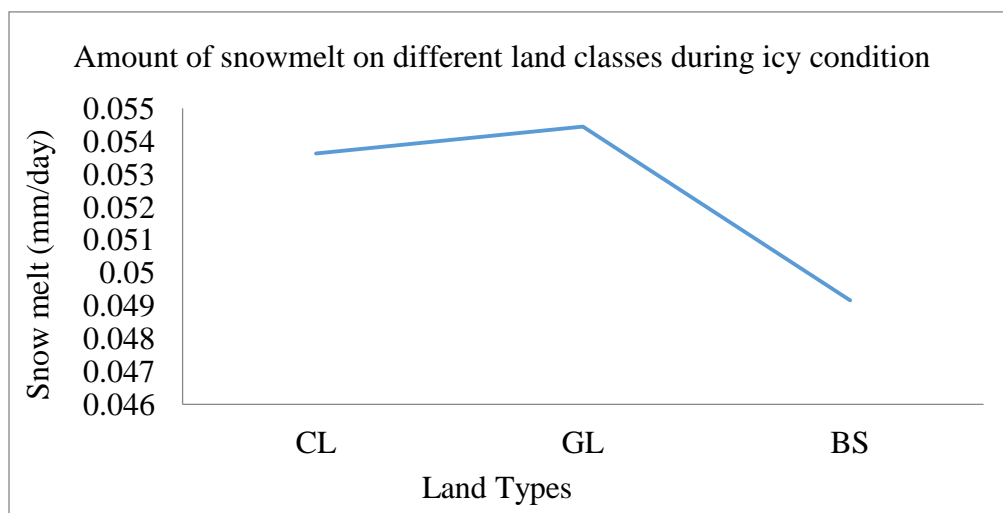
Figure 22. During icy condition amounts of snowmelt across cropland (CL), grassland (GL) and barren surface (BS) on date 02/08/2019

Table 13

Additional Snow Metamorphism Characteristics Chat for cropland, grassland and barren surface

Parameters	Cropland	Grassland	Barren Surface
Snow Density (kg/m^3)	317	319	365
Amount of Snowmelt (mm/day)	0.0536	0.0544	0.0491
Turbulent Flux	0.19	- 0.03	- 0.43
Snow Grain Size (mm)	0.5	1	2

During icy conditions the estimated amounts of snowmelt on three different land classes was found as follows- cropland: 0.0536 (mm/day); grassland: 0.0544 (mm/day) and barren surface: 0.0491(mm/day). The snow density was 317(kg/m^3) for cropland; 319(kg/m^3) for grassland and 365 (kg/m^3) on barren surface. The turbulent flux was estimated 0.19 on cropland; - 0.03 on grassland and - 0.43 on barren surface, and the snow grain sizes measured were 0.5mm on cropland; 1mm on grassland and 2mm on barren surface on that particular day. The average snow surface temperature was -18.4 (°C) on cropland; -15.1(°C) on grassland and -9.1 (°C) over barren surface. The average air temperature in the study area was -15.5(°C) on that specific day from 11:30am to 3:30pm respectively. This indicates that the snow surface temperature was lower than the air temperature. Thus, the cold content in the snow pack for three different land types was higher on that day making the snow to condense and retaining the snow temperature to

form ice respectively. However, more information were required to categories this type of snow metamorphism which was lacking in this study.

CHAPTER 5

DISCUSSION AND CONCLUSIONS

5.1 Discussion

In this study, change in snow density with respect to grain size of the snow during different field days across grassland, cropland and barren surface revealed variation in snow properties that supports Colbeck (1987) research on snow. Evolution of snow during different field days observed in this study also supports the findings from Choudhury and Chang (1981) research. Spatial heterogeneity of winter snow with space and time observed in this study was already found by Schmid et al. (2012) in their research. The tendency of snow pack to metamorphose constantly observed from this study was mentioned by Colbeck (1987), Wen et al. (2014), Fabienne (2012) and DeWalle and Rango (2008) in their studies. Moreover, even distribution and accumulation of snow with space and time observed from this study was found by Lemke et al. (2007) in their research. More likely, unstable weather conditions such as periodic snowfalls, precipitation, temperature fluctuation, wind speed, relative humidity, radiant fluxes and to some extent turbulent heat fluxes had influenced snow metamorphism characteristics across different land types in this research which supports Haeberli and Whiteman (2015) and Cline et al. (1998) studies. These components caused variation in estimated amounts of snowmelt on different field days in different land types in this study. Result from this research indicated net radiation flux played a crucial role in snow metamorphism in three different classes of land that supports the research done by Cline (1997) and Datt et al. (2008) on snow metamorphism. Densification of snowpack and

increase in the snow grain size observed during different field days clearly indicated that snow reduced its surface free energy which was found by Colbeck (1987) in his study. The decrease in snow pack density observed in this research due to large portion of the volumetric content in snow pack gets filled up with air supports study conducted by Rasmus (2005) in seasonal snow cover. In the study area different snow layers were observed that differed from each other but possesses relatively homogenous properties inside the layers caused by different snow metamorphoses which changed the size and shape of the snow grains was found by Rasmus (2005) in his study. Datt et al. (2008) found that the primary reason for variation in the size of snow particles was temperature and more absorption of solar radiation that increase the thermal state of snowpack was evidenced from this study. Additional heat flux in the snowpack was due to the turbulent fluxes that showed an increasing-decreasing pattern in this study reveals unstable conditions over snow pack in three different land types. In this study, the magnitude of turbulent flux gets largely influenced by the air mass characteristics affecting the surrounding wind speed, atmospheric temperature and moisture content as explained by Cline (1997) in his research was observed. Through this study, it was found that net radiation flux dominated over the turbulent flux for exchange of energy which was noticed by Boudhar et al. (2016) in their study. Results also indicated an increase in net radiation flux with the progress in field days during the study period. And according to Coakley (2003) research the net radiation flux energizes the turbulent heat exchange between the surface and the lowest layer of the atmosphere causing the snow to melt. The results from cumulative snowmelt from different land classes under study reveled that

melting of snow added surface water input into its surrounding which supports the findings of Tarboton et al. (1995).

In this research, the surrounding air temperature and the snow surface temperature during field data collection time on particular dates remains below 0 (°C) which was typically a freezing temperature. In this condition the snow particles gets filled-up with air and water vapour to form dry snow as according to a study by Endrizzi (2007). This contradicted the snow types found in this research when classified according to Seibert et al. (2015) snow categories. The results showed for both grassland and cropland 73% of the snow belongs to settled snow and 27% of the snow was wet snow, whereas, in barren surface it was found 45% of the snow belongs to settled snow and 55% of the snow was wet snow during the data collection days. Although the results showed that with the increase in snow grain size the average snow density increased across different land types, but in the case of barren surface the snow density was found to decrease at 1mm grain size contradicting the statement given by Judson and Doesken (2000) that snow density and the grain size were perfectly correlated. According to Colbeck (1987) the variations in snow grain size cause due to snow crystal modification when thermodynamics phase-equilibrium state were reached. Sturm and Holmgren (1995) stated the reason behind the increase in snow density was due to the influences of environmental variables such as temperature, snow depth, wind and heat flux which was evidenced from this research. Every new weather event had amplified the microstructure of snow in cropland, grassland and barren surface was found in this research that supports the studies done by Colbeck (1982) and Greene (2007) on snow evolution. Furthermore,

from this study it was also evident that snow properties greatly varies in space and time with relation to short-term weather condition like precipitation and air temperature change that made it easily eroded, transported and re-deposited by wind energy supports Haeberli and Whiteman (2015) research. Apart from this, Pomeroy and Brun (2001) had mentioned in their research that terrain features affects the variation in snow accumulation by trapping wind-transported snow in the open environments had been observed in this research. Hence, together all of these reasons had caused difference in snow density and snow grain size in this research respectively.

In this study, both the statistical analysis- ANOVA and T-test showed that there were no significant difference in the estimated amounts of snowmelt among the three land types under study. This can be attributed to several factors, such as limited sample size and inability to account for certain surface characteristics (slope, elevation). Further research is necessary to ascertain the potential differences of snowmelt among land cover classes.

This study also demonstrated that grain size was inversely related to the reflectance of the snow which supports the findings by Singh et al. (2005) and Singh et al. (2010) in their research. Hyvärinen and Lammasniemi (1987) also found that reflectance of snow was strongly dependent on snow grain size and the spectral variations in the ice absorption coefficient which was observed in this research. O'Brien and Munis (1975) observed from their research that snow possesses a distinctive spectral signature very high reflectance in the visible (VNIR) region which was noticed from this study. Moreover, high reflectance from snow particles were also found in SWIR1 region when

considered different snow grain size from different land types from different field days. The reason was explained by Negi et al. (2006) in their research in the upper Indian Himalaya during the winter seasons of the years 2004–2005 and 2005–2006. They found with the increase in contamination the peak of snow reflectance in the visible region gets shifted toward the higher wavelength range i.e., towards SWIR region.

In respect to the hyperspectral properties of snow, this study collected too few samples to characterize the differences between land cover classes and snow metamorphism stages. However, this work was able to identify key spectral ranges for hyperspectral snow characterization that could be used in further analysis. PCA that was applied to combine datasets collected during different dates with ASD FIeldSpec 3 spectroradiometer to attain an acceptable sample size, revealed components 1 and 2 with the following hyperspectral bands with component loadings > 0.9: 1014.5, 1024.5, 1034.5, and 355, 356, 374.5 and 394.5 nm respectively. This means that within the wavelength 350nm – 1039nm these bands are important for identifying snow metamorphism characteristics in grassland, cropland and barren surface irrespective of snow grain size.

If we place these findings in the context of the existing literature, they seem to correspond well with the earlier observations while providing an additional data reference point for hyperspectral imaging of snow. In particular, reflectance of freshly fallen snow generally varies more in the red end of the visible spectrum which declines in the shortwave infrared region (SWIR) at 1700 nm where there were minor peaks at approximately 1090–1100 nm noticed by O'Brien and Munis (1975) and Bolsenga and

Kistler (1982) from their research. And Wiscombe and Warren (1980) also observed the same kind of minor peak in the reflectance spectra of snow but at different wavelengths between 1830nm to 2240 nm having a strong depression in reflectance at 1950 and 2050 nm wavelength which was later argued by Warren (1982) in a study was due to contamination in snow. Singh et al. (2005) in their research found strong reflectance of snow in visible region of the wavelength that decrease gradually and become insignificant in SWIR region. Beside this they found minor peaks near 1100nm, 1300nm, 1800nm and 2200nm wavelength with a strong depression near 1950nm and 2050nm wavelength and the NIR showed reduction in peak which was centered at 1050nm and 1350. They also observed with the increase in grain size of the snow the spectral reflectance of snow deceases considerably the lowest was at 7 and < 8 with 1-2 mm grain size followed by < 1mm grain size at 8 and < 0.5mm grain size at < 9. In this study, major and minor peaks of snow reflectance were observed between the wavelengths 350nm to 1350nm approximately across cropland, grassland and barren surface according to grain size (.5mm, 1mm and 2mm) change respectively which contradict with the above mentioned researches done by various authors in different places. Also, it was found from this research that the lowest reflectance was > 1 at 2mm grain size in barren surface, > 2 at 1mm grain size in cropland and a reflectance of 2 at 1mm grain size in grassland. Again, the highest reflectance of snow was found > 8 at .5mm in grassland, a reflectance of 9 at .5mm grain size in cropland and a reflectance of < 8 at .5mm grain size in barren surface on different field days respectively which indicates snow ablation and increase in snow contamination.

Also, when Singh et al. (2010) analyzed their snow reflectance data collected from spectroradiometer at the Beas Basin they found band absorption depth at 1025nm increases with the increase in snow grain size. In this research, the highest bands absorption depth found in component 1 were 1014.5, 1024.5 and 1034.5, whereas, in component 2 the highest bands absorption depth were found in 355, 365, 374.5, 384.5 and 394.5 nm respectively after PCA analysis was carried out in different wavelengths considering different spectral data sets of snow reflectance taken on different field days for varied snow grain sizes across cropland, grassland and barren surface respectively.

5.2. Conclusions

Referring back to my hypothesis, the estimated amounts of snowmelt in this study was statistically insignificant across grassland, cropland and barren surface. There was no significant difference in the snowmelt in three different land classes which does not support the hypothesis of this research. With respect to the research questions proposed at the beginning of this study, the conclusions are as follows.

Can snow metamorphism be estimated from ground based investigation using physical properties of snow across cropland, grassland and barren surface? From the results it can be concluded that considering the snow metamorphism characteristics i.e., amounts of snowmelt along different grain sizes snow metamorphism can be estimated across grassland, cropland and barren surface with ground based investigation using physical properties of snow. The changing weather conditions altered the snowpack and simultaneously influenced the snow metamorphism characteristics respectively. Variation in density in snowpack across different land types on different days in this study indicates

melting and densification caused by increase – decrease in snow surface temperature (or cold contents) and surrounding air temperature as found in the result. Again, the reason for decrease in snow density in barren surface compared to grassland and cropland when the snow grain size was 1mm was likely due to trapped air inside the snowpack that increased the volume of the snow pack and relatively decreases the mass content in it. Because the elevation of barren surface was higher than grassland and cropland the prevalent wind blowing over barren surface was faster and air got trapped in the snow pack and deposited new snow composed of high percentage of air trapped over the accumulated snow crystals reduced the snow density.

Do the characteristics of snow metamorphism vary between cropland, grassland and barren surface? The statistical analysis results showed that there was no statistical difference in the estimated amounts of snowmelt between cropland, grassland and barren surface respectively.

Can ground based hyperspectral imaging detect differences in snow metamorphism characteristic between cropland, grassland and barren surface? In respect to the spectral reflectance of snow according to different grain size on different dates the results showed a considerable amount of variation between the three classes of lands under study respectively. Reduction in snow spectral reflectance in barren surface compared to cropland and grassland with different grain size on different field days was because of more contamination and increase in cold contents that transform the molten snow particles into ice by re-freezing it and reducing its albedo. Moreover, PCA analysis of snow reflectance datasets showed hyperspectral bands 1014.5, 1024.5, 1034.5, 355,

356, 374.5 and 394.5 nm were important to identify snow metamorphism characteristics across cropland, grassland and barren surface irrespective of grain size, land types and days of data collection respectively. Hence, it can be concluded that ground based hyperspectal imaging can efficiently detect snow metamorphism in cropland, grassland and barren surface.

Lastly, the ice-ground like formation was observed on date 02/08/2019 across cropland, grassland and barren surface that need further investigation and adequate data to compare from normal snow covered data. It can be assumed that more absorption of solar radiation had increased the thermal state of snowpack causing the snow to melt and low average snow temperature in different land type on that particular day had rapidly densified the snow pack as mentioned by Datt et al. (2008) in their study that converted the snow into ice.in this study. But due to deficit amount of data not much could be inferred from this research about this type of condition i.e., whether it was "ice-crust" or "melt-freeze" metamorphism.

5.3. Limitations of the Study

Weather conditions such as wind blowing > 10 mph, cloudiness > 40%, snowfall, rainfall and temperature below 0 degree Fahrenheit were not considered in this study because it creates problems in field data collection procedure. Contamination due to soil, dust and shoots deposition were neglected in this research, although snow reflectance and snow albedo gets heavily affected by the contaminants (Hansen & Nazarenko, 2004; Painter et al., 2005). Mean snow albedo value .66 was used in this research to calculate shortwave radiation in the study area as used by Cline (1997); Briegleb et al. (1986) in

their study. Beside this, mean values for heat transfer coefficient and humidity transfer coefficient were used in this study. Ground flux and precipitation data were not consider in the snow surface energy flux equation due to its negligible effect on snowmelt according to Obled and Harder (1979); Male and Granger (1981) in their study. Other factors such as, elevation, slope, aspect were not taken into consideration in this research.

5.4. Future Directions

In future, if this work is to be continued then ground factors such as slope, elevation and aspects will be used to understand how these factors affect the accumulation and depth of snow at different land classes. Daily data of snowpack physical properties will be collected regardless of any weather conditions to study snow metamorphism on grassland, cropland and barren surface respectively. Heat transfer coefficient and humidity transfer coefficient will be calculated individually to use it in the energy flux model. Snow reflectance data with field spectroradiometer from different locations at different height per day will be used to identify snow metamorphism characteristics over cropland, grassland and barren surface respectively. The current snow energy flux model developed in this study will be used to study snow metamorphism on other locations to check the generality of the model. Additionally, a model comparison with other snow energy fluxes models will to be done to validate statistical significance of the model used in this study. Ground heat transfer and rainfall data will be included in the snow energy flux model to identify differences in snow metamorphism (if any) across cropland, grassland and barren surface. Additionally, snow water equivalent will be calculated for different land types to understand the water contain within snowpack to

include in the result. Snow surface albedo will be measured as because it is a key ingredient in remote sensing of snow top and atmospheric properties from space (Coakley, 2003). And it depends upon the wavelength, zenith angle, snow grain size, impurity content and cloud cover which are very important for measuring snow melting and snow energy balance at the surface (Warren, 1982). Also, different phase change in snow metamorphism or different stages of snow metamorphism will be another potential study to perform to understand snow metamorphism could be considered for future research. Lastly, different airborne hyperspectral images over different land classes could be used along with spectral data from spectroradiometer of snow reflectance to relate with snow metamorphism characteristics to study snow metamorphism respectively.

REFERENCES

Adolph, A. C., Albert, M. R., Lazarcik, J., Dibb, J. E., Amante, J. M., & Price, A. (2017). Dominance of grain size impacts on seasonal snow albedo at open sites in New Hampshire. *J. Geophys. Res. Atmos., 122,* 121–139. doi:10.1002/ 2016JD025362.

Akyurek, Z., & Sorman, A. U. (2002). Monitoring snow covered area using NOAA-AVHRR data in the eastern part of Turkey. *Hydrological Science, 47,* 243-252. doi: 10.1080/02626660209492927.

Albert, M. R., Hardy, J. P., & Marsh, P. (1993). An introduction to snow hydrology and its integration with physical, chemical and biological systems. In J. Hardy, M. R. Albert, & P. Marsh (Eds.), *Snow hydrology: The integration of physical chemical and biological systems* (373). John Wiley and Sons.

Analytical Spectral Devices. (1999). *Fieldspec TM: Technical guide* (3rd ed.). Boulder, CO, USA: Analytical Spectral Devices.

Andresen, J., Hilberg, S., & Kunkel, K. (2012). Historical climate and climate trends in the Midwestern USA. In J. Winkler, J. Andresen, J. Hatfield, D. Bidwell, & D. Brown (coordinators), *U.S. National Climate Assessment Midwest Technical Input Report*. Available from the Great Lakes Integrated Sciences and Assessments (GLISA) Center. Retrieved from http://glisa.msu.edu/docs/NCA/MTIT_Historical.pdf.

Arey, M. F. (1906). Geology of Black Hawk County. In *Iowa Geological Survey* (Annual Report 1905, 16, 409-452). Retrieved from https://ir.uiowa.edu/cgi/viewcontent.cgi?article=1100&context=igsar

ASD Inc. (2010). *FieldSpec $^®$ 3 user manual* (ASD Document 600540). Retrieved from www.asdi.com.

Barnett, T. P., Adam, J. C., & Lettenmaier, D. P. (2005). Potential impacts of a warming climate on water availability in snow dominated regions. *Nature, 438*(7066), 303–309. doi: 10.1038/nature04141.

Barnaby, I. (1980). *Snowmelt observations in Alberta.* 48th Western Snow Conference.

Benestad, R. E. (2005). Climate change scenarios for Northern Europe from multi-model IPCC AR4 climate simulations. *Geophysical Research Letters, 32*(17). L17704. doi: https://doi.org/10.1029/2005GL023401

Beria, H., Larsen, J. R., Ceperley, N. C., Michelon, A., Vennemann, T., & Schaefli, B. (2018). Understanding snow hydrological processes through the lens of stable water isotopes. *Wiley Interdisciplinary Reviews: Water, 5*(6), e1311. doi: https://doi.org/10.1002/wat2.1311

Bigelow, D. (2017, December 4). A Primer in land use in the United States. *Amber Waves Magazine*. Retrieved from https://www.ers.usda.gov/amber-waves/2017/december/a-primer-on-land-use-in-the-united-states/

Blöschl, G., Hall, J., Parajka, J., Perdigão, R. A. P., Merz, B., Arheimer,B., ... Zivkovic, N. (2017). Changing climate shifts timing of European floods. *Science, 357*(6351)*,* 588–590. doi: https://doi.org/10.1126/science.aan2506

Bolsenga, S. J., & Kistler, R. D. (1982). A dual spectroradiometer system for measuring spectral reflectance. *Journal of Applied Meteorology, 21,* 642–647.

Boudhar, A., Boulet, G., Hanich, L., Sicart, J. E., & Chehbouni, A. (2016). Energy fluxes and melt rate of a seasonal snow cover in the Moroccan High Atlas. *Hydrological Sciences Journal, 61*(5)*,* 931-943. doi: 10.1080/02626667.2014.965173

Brodzik, M. J., & Armstrong, R. (2017). Northern Hemisphere EASE-Grid 2.0 weekly snow cover and sea ice extent, Version 4. *NASA National Snow and Ice Data Center Distributed Active Archive Center.* Boulder, Colorado, USA.

Briegleb, B. P., Minnis, P., Ramanathan, V., & Harrison, E. (1986). Comparison of regional clear-sky albedos inferred from satellite observations and model computations. *Journal of Climate and Applied Meteorology, 25,* 214 – 226.

Brun, E., Martin, E., Gendre, V. S. C., & Coleou, C. (1989). An energy and mass model of snow cover suitable for operational avalanche forecasting. *Journal of Glaciology, 35,* 333–342.

Bryant, A., & Painter, T. (2010). *Radiative forcing by dust in snowmelt-dominated hydrologic systems using coupled satellite and in-situ measurements.*78th Western Snow Conference, 43–47.

Buchmiller, R. C., & Eash, D. A. (2010). *Floods of May and June 2008 in Iowa, U.S.* (Annual Report 2010–1096, 10). Retrieved from https://pubs.usgs.gov/of/2010/1096/

Callaghan, T. V., & Johansson, M. (2014). Snow, ice and the biosphere. In W. Haeberli, & C. Whiteman (Eds.), *Snow and ice-related hazards, risks and disasters* (39 -165). Elsevier.

Chamberlain, D., & Tighe, M. L. (2009). *Land Cover Classification: A comparison between U.S. National Land Cover Dataset (NLCD) and INTERMAP'S NEXTMAP USA derived land cover maps.* In Proceedings of the ASPRS/MAPPS Fall Conference (16–19), San Antonio, TX, USA.

Chen, X., Liang, S., Cao, Y., He, T., & Wang, D. (2015). Observed contrast changes in snow cover phenology in northern middle and high latitudes from 2001–2014. *Scientific Reports, 5,* 16820. Retrieved from https://www.semanticscholar.org/paper/Observed-contrast-changes-in-snow-cover-phenology-Chen-Liang/1881c8c3b771e5f73c016926aac7a0f788ef20a9/abstract

Chen, F., Barlagel, M., Tewari, M., Rasmussen, R., Jin, J., Lettenmaier, D., ... Yang, Z. L. (2014). Modeling seasonal snowpack evolution in the complex terrain and forested Colorado Headwaters region: A model intercomparison study. *J. Geophys. Res. Atmos.,* 119. doi:10.1002/2014JD022167.

Choudhury, B. J., & Chang, A. T. (1981). The albedo of snow for partially cloudy skies Boundary Layer. *Meteorology, 20,* 371—389.

Clark, R. N., Swayze G. A., Livo, K. E., Kokaly, R. F, King, J. B., Dalton, J. S., ... McDougal, R. R. (2002). Surface reflectance calibration of terrestrial Imaging Spectroscopy Data: A Tutorial using AVIRIS. Retrieved from http://speclab.cr.usgs.gov/ PAPERS.calibration.tutorial

Clark, R. N. (1999). Spectroscopy of rocks and minerals, and principles of spectroscopy. In A. N. Rencz (Ed.), *Remote sensing for the earth sciences* (3–58). John Wiley & Sons. Retrieved from https://pdfs.semanticscholar.org/1e02/a41e9ff88cdf80bbe41bd81ecde71e779548.pdf?_ga=2.246577795.665514673.1592461352-1289527414.1553051090

Clark, R. N., Swayze, G. A., Gallagher, A. J., Trude, V. V. K., & Calvin, W. M. (1993). *The U. S. Geological Survey, Digital Spectral Library: Version 1 (0.2 to 3.0um).* (Open-File Report 93-592). doi: https://doi.org/10.3133/ofr93592

Clark, R. N., & Roush, T. L. (1984). Reflectance spectroscopy: Quantitative analysis techniques for remote sensing applications. *J Geophys Res., 89* (B7), 6329–6340.

Cline, D. W., Bales, R. C., & Dozier, J. (1998). Estimating the spatial distribution of snow in mountain basins using remote sensing and energy balance modeling. *Water Resources Research, 34*(5), 1275–1285. doi. https://doi.org/10.1029/97WR03755.

Cline, D. W. (1997). Snow surface energy exchanges and snowmelt at a continental mid-latitude Alpine site. *Water Resources Research, 33*(4), 689-701.

Coakley, J. A. (2003). Reflectance and Albedo, Surface. In J. R. Holton, J. A. Curry, J. A. Pyle (Eds.), *Encyclopedia of the atmospheric science* (1914-1923). Academic Press. Retrieved from https://curry.eas.gatech.edu/Courses/6140/ency/Chapter9/Ency_Atmos/Reflectance_Albedo_Surface.pdf

Colbeck, S. C., & Jamieson, J. B. (2001). The formation of faceted layers above crusts. *Cold Regions Science and Technology, 33,* 247-252.

Colbeck, S. C. (1987). A review of the metamorphism and classification of seasonal snow crystal. *IAHS Publication, 162,* 3–24.

Colbeck, S. C. (1983). Theory of metamorphism of dry snow. *Journal of Geophysical Research, 88,* 5475–5482.

Colbeck, S. C. (1982). An overview of seasonal snow metamorphism. *Rev. Geophys. Space Phys., 20*(1)*,* 45–61. doi: 10.1029/ RG020i001p00045

Curtiss, B., & Goetz, A. F. H. (1994, July 10-15). *Field spectrometry: Techniques and instrumentation.* In Proceedings of an International Symposium on Spectral Sensing Research (31-40), San Diego, California, USA.

Daly, S. F., Davis, R., Ochs, E., & Pangburn, T. (2000). An approach to spatially distributed snow modelling of the Sacramento and San Joaquin Basins, California. *Hydrol. Process., 14*(18)*,* 3257–3271. doi: https://doi.org/10.1002/1099-1085(20001230)14:18<3257::AID-HYP199>3.0.CO;2-Z.

Danner, M., Locherer, M., Hank, T., & Richter, K. (2015). *Spectral sampling with the ASD FieldSpec 4 – Theory, Measurement, Problems, Interpretation.* In EnMAP Field Guides Technical Report. *GFZ Data Services*. doi: http://doi.org/10.2312/enmap.2015.008

Datt, P., Srivastava, P. K., Negi, P. S., & Satyawali, P. K. (2008). Surface energy balance of seasonal snow cover for snow-melt estimation in N–W Himalaya. *Journal of Earth System Science, 117*(5)*,* 567–573.

Davis, R., Pangburn, T., Daly, S., Ochs, E., Hardy, J. P., Bryant, E., & Pugner, P. (1999). *Can satellite snow maps, ground measurements and modeling improve water management and control in the King's River Basin, California- Efforts toward finding the answer.* 67th Western Snow Conference, 54–61. Retrieved from https://westernsnowconference.org/sites/westernsnowconference.org/PDFs/1999Davis.pdf

Deardroff, J. W. (1968). Dependence of air sea transfer coefficients on bulk stability. *J. Geophys. Res., 73*(8), 2549 – 2557.

Derksen, C., & Brown, R. (2012). Spring snow cover extent reductions in the 2008–2012 period exceeding climate model projections. *Geophysical Research Letter*, *39*(19). L19504, 1–6. doi: https://doi.org/10.1029/2012GL053387

DeWalle, D. R., & Rango, A. (2008). *Principles of snow hydrology*. Cambridge University Press. doi: https://doi.org/10.1017/CBO9780511535673

Dimopoulos, I. (2017). *Classification using hyper-spectral imagery* [Master's thesis]. Technological Education Institute of Piraeus.

Dingman, S. L. (2015). *Physical hydrology* (3rd ed.). Waveland Press.

Dingman, S. L. (1994). *Physical hydrology*. MacMillan Publishing Company.

Dozier, J. (2011). Mountain hydrology, snow color, and the fourth paradigm. *Eos Trans. AGU, 92*(43), 373–374. doi:10.1029/2011EO430001.

Dozier, J., Green, R. O., Nolin, A.W., & Painter, T. H. (2009). Interpretation of snow properties from imaging spectrometry. *Remote Sensing of Environment, 113,* S25-S37. doi: https://doi.org/10.1016/j.rse.2007.07.029.

Dozier, J., & Painter, T. H. (2004). Multispectral and hyperspectral remote sensing of Alpine snow properties. *Annu. Rev. Earth Planet. Sci., 32*(1), 465–494. doi: https://doi.org/10.1146/annurev.earth.32.101802.120404, 2004.

Dutta, D., Mahalakshmi, D. V., Singh, M., Goyal, P., Paul, S., Jaswant Raj Sharma, J. R., & Dadhwal, V. K. (2015). Satellite-based estimation of instantaneous radiative fluxes over continental USA – a Case Study. *Journal of Indian Society of Remote Sensing, 43*(4),1 – 9. doi: 10.1007/s12524-015-0449-1

Dudley, K. L., Dennison, P. E., Roth, K. L., Roberts, D. A., & Coates, A. R. (2015). A multi-temporal spectral library approach for mapping vegetation species across spatial and temporal phenological gradients. *Remote Sensing of Environment, 167,* 121-134. doi: https://doi.org/10.1016/j.rse.2015.05.004.

Endrizzi, S. (2007). *Snow cover modelling at a local and distributed scale over complex terrain* [Doctoral dissertation]. Environmental Engineering XIX cycle. Retrieved from http://www.erdc.usace.army.mil/pls/erdcpub/docs/erdc/images/ SNTHERM.pd

Essery, R. (2003). Aggregated and distributed modelling of snow cover for a high-latitude basin. *Glob. Planet. Change, 38,* 115 - 120.

Fabienne, R. (2012). *Snow metamorphism affected by thermal conductivity and grain boundaries* [Doctoral dissertation]. ETH Zurich, Zurich, Switzerland. doi. https://doi.org/10.3929/ethz-a-007575926

Fassnacht, S. R., Helfrich, S., Lampkin, D., Dressler, K., Bales, R., Halper, E., ... Imam, B. (2001). *Snowpack modelling of the Salt Basin with water management implications.* In Proceedings of the Western Snow Conference, 69, (65–76).

Fierz, C., Armstrong, R. L., Durand, Y., Etchevers, P., Greene, E., McClung, D. M., ... Sokratov, S. A. (2009). *The international classification for seasonal snow on the ground* (IHP Technical Documents in Hydrology 83). UNESCO–International Hydrological Programme, Paris. Retrieved from https://unesdoc.unesco.org/ark:/48223/pf0000186462

Flanner, M. G., & Zender, C. S. (2006). Linking snowpack microphysics and albedo evolution. *Journal of Geophysical Research, 3,* DI2208. doi:10.1029/2005JD006834.

Foley, J. A., Ramankutty, N., Brauman, K. A., Cassidy, E. S., Gerber, J. S., Johnston, M., ... Balzer, C. (2011). Solutions for a cultivated planet. *Nature, 478* (7369), 337.

Forbes, M. H. (2019, March 15). Rain, melting snow causes flooding in Cedar Falls' North Cedar neighborhood. *The Courier.* Retrieved from https://wcfcourier.com/news/local/gravel-roads-a-wet-muddy-mess-parks-closed-to-flooding/article_151446fa-90a5-5a6d-91eb-b8bb7f088f56.html

Fountanas, L. (2004). *Principal components based techniques for hyperspectral Image data* [Master's thesis]. Naval Postgraduate School, Monterey, California. Retrieved from http://hdl.handle.net/10945/1266

Frei, A., Tedesco, M., Lee, S., Foster, J., Hall, D. K., Kelly, R., & Robinson, D. A. (2012). A review of global satellite-derived snow products. *Advances in Space Research, 50*(8), 1007–1029. doi: https://doi.org/10.1016/j.asr.2011.12.021

Freudiger, D., Kohn, I., Stahl, K., & Weiler, M. (2014). Large-scale analysis of changing frequencies of rain-on-snow events with flood-generation potential. *Hydrology and Earth System Sciences, 18*(7), 2695–2709. doi: https://doi.org/10.5194/hess-18-2695-2014

Garfagnoli, F., Martelloni, G., Ciampalini, A., Innocenti, L., & Moretti, S. (2013). Two GUIs – based analysis tool for spectroradiometer data pre-processing. *Earth Science Informatics, 6* (4)*,* 227 – 240. doi: 10.1007/s12145-013-0124-4

Goetz, A. F. H., Vane, G., Solomon, J. E., & Rock, B. N. (1985). Imaging spectrometry for Earth remote sensing. *Science, 228*, 1147-1153. doi: http://doi.org/10.1126/science.228.4704.1147.

Gray, D. M., & Male, D. H. (1981). *Handbook of snow, principles, processes, management and use.* Pergamon Press.

Gray, D., & Landine, P. (1988). An energy-budget snowmelt model for the Canadian Prairies. *Can. J. Earth Science, 25*(8), 1292–1303.

Green, A. A., & Craig, M. D. (1985). *Analysis of aircraft spectrometer data with logarithmic residuals*. In JPL Proceedings of The Airborne Imaging Spectrometer Data Analysis Workshop (111–119). Retrieved from https://ntrs.nasa.gov/ archive/nasa/casi.ntrs.nasa.gov/19860002169.pdf

Greene, E. M. (2007). *The thermophysical and microstructural effects of an artificial ice layer in natural snow under kinetic growth metamorphism* [Doctoral dissertation]. Colorado State University. US. Retrieved from https://www.researchgate.net/ publication/234472805_The_thermophysical_and_microstructural_effects_of_an_ artificial_ice_layer_in_natural_snow_under_kinetic_growth_metamorphism

Gustafsson, D., Stahli, M., & Jansson, P. E. (2001). The surface energy balance of a snow cover: Comparing measurements to two different simulation models. *Theoretical and Applied Climatology, 70,* 81–96. doi: 10.1007/s007040170007.

Haeberli, W., & Whiteman, C. (2015). Snow and ice- related hazards, risks, and disasters: A general framework. In *Snow and ice-related hazards, risks and disasters* (1-34). doi. 10.1016/B978-0-12-394849-6.00001-9

Hall, D. K., Riggs, G. A., & Salomonson, V. V. (1995). Development of methods for mapping global snow cover using moderate resolution imaging spectroradiometer data. *Remote Sensing of Environment*, *54,* 127–140.

Hansen, J., & Nazarenko, L. (2004). Soot climate forcing via snow and ice albedos. *Proc. Natl. Acad. Sci.*, *101*(2), 423–428. doi: 10.1073/ pnas.2237157100.

Harr, R. (1981). Some characteristics and consequences of snowmelt during rainfall in western Oregon. *Journal of Hydrology, 53,* 277–304.

Harshburger, B., Blandford, T., Humes, K., Walden, V., & Moore, B. (2005). *Evaluation of enhancements to the snowmelt runoff model.* In Proc. Western Snow Conf. (57–63).

Hasebe, M., & Kumekawa, T. (1995). Estimation of snowmelt volume using air temperature and wind speed. *Environment International, 21*(5)*,* 497 -500. doi: https://doi.org/10.1016/0160-4120(95)00048-P

Herold, M., Roberts, D. A., Gardner, M. E., & Dennison, P. E. (2004). Spectrometry for urban area remote sensing—Development and analysis of a spectral library from 350 to 2400 nm. *Remote Sensing of Environment, 91*(3-4)*,* 304-319. doi: https://doi.org/10.1016/j.rse.2004.02.013

Homer, C., Dewitz, J., Jim, S., Xian, G., Costello, C., Danielson, P., ... Riitters, K. (2020). Conterminous United States land cover change patterns 2001–2016 from the 2016 National Land Cover Database. *ISPRS Journal of Photogrammetry and Remote Sensing, 162,* 184 – 199. doi. https://doi.org/10.1016/j.isprsjprs.2020.02.019

Homer, C., Dewitz, J., Fry, J., Coan, M., Hossain, N., Larson, C., ... Wickham, J. (2007). Completion of the 2001 National Land Cover database for the conterminous United States. *Photogrammetric Engineering and Remote Sensing, 73*(4), 337 – 341. Retrieved from https://www.researchgate.net/publication/237239863

Hong, M., Zongchao, L., & Yifeng, L. (1992). Energy balance of snow cover and simulation of snow-melt in the western Tien Shan mountains, China. *Ann. Glaciol., 16,* 73–78.

Hueni, A., & Tuohy, M. (2006). Spectroradiometer data structuring, pre-processing and analysis–An IT based approach. *Spatial Science*, *52*(2), 93-102. doi: 10.1080/14498596.2006.9635084.

Hyvärinen, T., & Lammasniemi, J. (1987). Infrared measurement of free-water content and Grain Size of Snow. *Optical Engineering, 26*(4), 342-48.

Jain, S. K., Goswami, A., & Saraf, A. K. (2008). Accuracy assessment of MODIS, NOAA and IRS data in snow cover mapping under Himalayan conditions. *International Journal of Remote Sensing*, *29,* 5863–5878.

Jaoumot, J., Gargallo, R., de Juan, A., & Tauler, R. (2005). A graphical user friendly interface for MCR ALS: A new tool for multivariate curve resolution in MATLAB. *Chemom Intell Lab Syst., 76*, 101–110.

Jordan, R. (1991). A one-dimentional temperature model for a snow cover: Technical documentation for SNTHERM (89). *U.S. Army Corps of Engineers, Special Report, 91-16.* Available from Regions Research and Engineering Laboratory, Hanover, HN.

Judson, A., & Doesken, N. (2000). Density of freshly fallen snow in the Central Rocky Mountains. *Bulletin of the American Meteorological Society, 81*(7), 1577-1588. doi: https://doi.org/10.1175/1520-0477(2000)081<1577:DOFFSI>2.3.CO;2

Karl, T. R., & Trenberth, K. E. (2003). Modern global climate change. *Science, 302,* 1719–1723. doi: 10.1126/science.1090228.

Kay, J. E. (2006, April). *Snow density observation in the Washington Cascades.* 74th Annual Western Snow Conference, Las Cruces, NM.

Kinar, N. J., & Pomeroy, J. W. (2015). Measurement of the physical properties of the snowpack. *Reviews of Geophysics, 53.* doi:10.1002/2015RG000481.

King, J., Pomeroy, J. W., Gray, D. M., Fierz, C., Föhn, P. M. B., Harding, R. J., ... Pluss, C. (2008). Snow atmosphere energy and mass balance. In R. L. Armstrong & E. Brun (Eds.), *Snow and climate: Physical processes, surface energy exchange and modeling* (70 – 125). Cambridge University Press. Retrieved from https://www.dora.lib4ri.ch/wsl/islandora/object/wsl:11837

Kirnbauer, R., Bloschl, G., & Gutknecht, D. (1994). Entering the era of distributed snow models. *Nord. Hydrol., 25*(1/2)*,* 1-24.

Klein, A. G., Hall, D. K., & Nolin, A. W. (2000, May 17-19). *Development of a prototype snow albedo algorithm for the NASA MODIS instrument.* 57th Eastern Snow Conference, 143–158, Sysacuse, NY, USA.

Koch, R., & Fisher, A. (2000). *Effects of inter-annual and decadal-scale climate variability on winter and spring stream flow in western Oregon and Washington.* In Proc. Western Snow Conference, 68, (1–11).

Krishna, S. S., Manavalan, P., & Rao, P. V. N. (2014). Estimation of net radiation using satellite-based data inputs. *Int. Arch. Photogramm. Remote Sens. Spat. Inf. Sci.,* *XL- 8*, 307–313. doi: 10.5194/isprsarchives-XL-8-307-2014

Kuester, M. A., Thome, K., Krause, K., Canham, K., & Whittington, E. (2001). *Comparison of surface reflectance measurements from three ASD FieldSpec FR Spectroradiometers and one ASDFieldSpec VNIR Spectroradiometer.* In IEEE International Geoscience & Remote Sensing Symposium. IEEE Xplore, Sydney, NSW, Australia. doi:10.1109/IGARSS.2001.976060

Kuusisto, E. (1986). The energy balance of a melting snow cover in different environments in modelling snowmelt-induced processes. *IAHS, 155,* 37-45.

Langlois, A., Bergeron, J., Brown, R., Royer, A., Harvet, R., Roy, A., … Theriault, N. (2014). Evaluation of CLASS 2.7 and 3.5 simulations of snow properties from the Canadian Regional Climate Model (CRCM4) over Quebec, Canada. *Journal of Hydrology, 15,* 1325 – 1343. doi. 10.1175/JHM-D-13-055.1

Lee, K. S., Jin, D., Yeom, J. M., Seo, M., Choi, S., Kim, J. J., & Han, K.S. (2017). New approach for snow cover detection through spectral pattern recognition with MODIS Data. *Journal of Sensors, 2017,* 15. doi. https://doi.org/10.1155/2017/4820905.

Lemke, P., Ren, J., Alley, R. B., Allison, I., Carrasco, J., Flato, G., … Zhang, T. (2007). Observations: Changes in snow, ice and frozen ground. In S. Solomon, D. Qin, M. Manning, Z. Chen, M. Marquis, K. B. Averyt, M. Tignor, & H. L. Miller (Eds.), *Climate change 2007: The physical science basis. Contribution of working group I to the fourth assessment report of the Intergovernmental Panel on Climate Change.* Cambridge University Press, Cambridge, United Kingdom and New York, NY, USA.

Leppanen, L., Kontu, A., Vehvilainen, J., Lemmetyinen, J., & Pulliainen, J. (2015). Comparison of traditional and optical grain-size field measurements with SNOWPACK simulations in a taiga snowpack. *Journal of Glaciology, 61*(225). doi: 10.3189/2015JoG14J026

Liston, G. E., & Hiemstra, C. A. (2011). The changing cryosphere: Pan-Arctic snow trends (1979–2009). *J. Climate, 24,* 5691–5712.

Lopez, M. G., Vis, M. J. P., Jenicek, M., Griessinger, N. & Seibert, J. (2020). Complexity and performance of temperature-based snow routines for runoff modelling in mountainous areas in Central Europe, *Hydrol. Earth Syst. Sci. Discuss.* doi: https://doi.org/10.5194/hess-2020-57.

Lu, H., Wei, W. S., Liu, M. Z., Han, X., Li, M., & Hong, W. (2016). Variation in seasonal snow surface energy exchange during a snowmelt period: As example from the Tianshan Mountain, China. *Meteorological Application, 23,* 14-25. doi: 10.1002/met.1511

Lundberg, A., Granlund, N., & Gustafsson, D. (2008, May). *"Ground truth" Snow measurements – Review of operational and new measurement methods for Sweden, Norway, and Finland.* In Proceedings of the 65th Annual Eastern Snow Conference, (NH: ERDC-CRREL, 215-237), Fairlee, Vermont, USA. Hanover.

MacDonald, L. H., & Stednick, J. D. (2003). Forests and water: A state-of-the-art review for Colorado. *Colorado Water Resources Research Institute,* 65. Colorado State Univ., Fort Collins.

Male, D. H., & Granger, R. J. (1981). Snow surface energy exchange. *Water Resources Research, 17,* 609–627. doi: 10.1029/ WR017i003p00609.

Malvern, F. (2014). Computing net radiation from temperature variables: Improvising for under-resourced weather stations in developing countries. *IOSR Journal of Applied Physics, 5*(5), 1 – 6. Retrieved from www.iosrjournals.org

Marks, D., Cooley, K., Robertson, D., & Winstral, A. (2001). Long-term snow database, Reynolds Creek Experimental Watershed, Idaho, United States. *Water Resource Research, 37*(11)*,* 2835–2838. doi: https://doi.org/10.1029/2001WR000416.

Marks, D., Domingo, J., Susong, D., Link, T., & Garen, D. (1999). A spatially distributed energy balance snowmelt model for application in mountain basins. *Hydrology Process., 13,* 1935–1959.

Marks, D., Kimball, J., Tingey, D., & Link, T. (1998). The sensitivity of snowmelt processes to climate conditions and forest cover during rain-on-snow: A case study of the 1996 Pacific Northwest flood. *Hydrological Processes, 12*(10– 11), 1569–1587.

Marpu, P. R., Pedergnana, M., Mura, M. D., Peeters, S., Benediktsson, J. A., & Bruzzone, L. (2012). Classification of hyperspectral data using extended attribute profiles based on supervised and unsupervised feature extraction techniques. *International Journal of Image and Data Fusion, 3*(3), 269–298. doi:10.1080/19479832.2012.702687

Marsh, P. (1990). Snow hydrology, in Northern Hydrology: Canadian Perspectives. In T. D. Prowse, & C. S. L. Ommanney (Eds.), *NHRI Science Rep., 1* (37–61). Natl. Water Res. Inst., Saskatoon, Canada.

Martin, E., & Lejeune, Y. (1998). Turbulent fluxes above the snow surface. *Ann. Glaciol., 26,* 179-183.

Merz, R., & Blöschl, G. (2003). A process typology of regional floods. *Water Resource Res., 39*(12), 1–20. doi: 10.1029/2002WR001952.

Mazurkiewicz, A. B., Callery, D. G., & McDonnell, J. J. (2008). Assessing the controls of the snow energy balance and water available for runoff in a rain-on-snow environment. *Journal of Hydrology, 354,* 1–14. doi:10.1016/j.jhydrol.2007.12.027.

Merzdorf, J. (2020, March 23). Solar energy tracker powers down after 17 years. *NASA's Goddard Space Flight Center*. Retrieved from https://climate.nasa.gov/news/2960/solar-energy-tracker-powers-down-after-17-years/

Meyfroidt, P., Chowdhury, R. R., de Bremond, A., Ellis, E. C., Erb, K. H., Filatova, T., ... Kull, C. A. (2018). Middle range theories of land system change. *Global Environ. Change, 53,* 52–67.

McCarthy, J. J., Canziani, O. F., Leary, N. A., Dokken, D. J., & White, K. S. (2001). *Climate change 2001: Impacts, adaptation and vulnerability*. Cambridge University Press. Retrieved from https://library.harvard.edu/collections/ipcc/docs/27_WGIITAR_FINAL.pdf

McKay, G., & Blackwell, S. (1961). *Plains snowpack water equivalent from climatological records.* 29th Annual Western Snow Conference, Spokane, Washington.

Milton, E. J., Schaepman, M. E., Anderson. K., Kneubühler, M., & Fox, N. (2009). Progress in field spectroscopy. *Remote Sens. Environ., 113,* 92-109.

Mote, P., Li, S., Letternaier, D., Xiao, M., & Engel, R. (2018). Dramatic declines in snowpack in the western US. *npj Climate and Atmospheric Science, 1,* 1–6. doi. https://doi.org/10.1038/s41612-018-0012-1.

Muñoz, J., Infante, J., Lakhankar, T., Khanbilvardi, R., Romanov, P., Krakauer, N., & Powell, A. I. (2013). Synergistic use of remote sensing for snow cover and snow water equivalent estimation. *British Journal of Environment & Climate Change, 3*(4), 612-627.

National Snow and Ice Data. (2020, January 10). Snow and climate. Retrieved from https://nsidc.org/cryosphere/snow/climate.html

Negi, H. S., Shekhar, C., & Singh, S. K. (2015). Snow and glacier investigations using hyperspectral data in the Himalaya. *Current Science, 208*(5), 892-902. Retrieved from https://www.researchgate.net/publication/281698682.

Negi, H. S., & Kokhanovsky, A. (2011). Retrieval of snow albedo and grain size using reflectance measurements in Himalayan basin. *The Cryosphere, 5,* 203–217. Retrieved from http://www.the-cryosphere.net/5/203/2011/.

Negi, H. S., Kulkarni, A. V., Prajapati, R. P., Singh, S. K., & Sharma, J. K. (2006). *Effect of contamination and mixed objects on snow reflectance using spectroradiometer.* (Report RSAM/SAC/RESIPA/MWRG-GLI/SN-25/2006). doi: 10.13140/RG.2.2.25443.14887

Negi, P. S., Semwal, G., Sethi, D. N., & Chand, U. (2004). A comparative study of snow-melt parameters, albedo and estimated surface energy budget of snow surface of Pir Panjal and Great Himalayan ranges of Indian Himalaya. *International Symposium on Snow Monitoring and Avalanches,* 567-571.

Nolin, A. W., & Dozier, J. (2000). A hyperspectral method for remotely sensing the grain size of snow. *Remote Sensing of Environment, 74*(2), 207-216. doi. 10.1016/S0034-4257(00)00111-5

Nolin, A. W. (2010). Recent advances in remote sensing of seasonal snow. *Journal of Glaciology, 56* (200)*,* 1141-1150. doi. https://doi.org/10.3189/ 002214311796406077

Nolin, A.W., & Stroeve, J. C. (1997). The changing albedo of the Greenland Ice Sheet: Implications for climate change. *Annals of Glaciology, 25,* 51-57.

Norman, V., & Karen, E. (1987). *A survey of the vascular flora of Black Hawk County, Iowa* [Master's thesis].University of Northern Iowa, Cedar Falls, Iowa. Retrieved from https://scholarworks.uni.edu/etd/194

Obled, C., & Harder, H. (1979, September 26-28). *A review of snow melt in the mountain environment.* In Proceedings of a Meeting on Modelling of Snow Cover Runoff (CRREL, 179 – 204), Hanover, New Hampshire.

O'Brien, H.W., & Munis, R. H. (1975). Red and near infrared reflectance of snow. *CRREL Research Report, 332,* 18. U.S. Army Cold Regions Research and Engineering Laboratory, Hanover, New Hampshire. Retrieved from https://ntrs.nasa.gov/archive/nasa/casi.ntrs.nasa.gov/19760009497.pdf

Painter, T. H., Barrett, A. P., Landry, C., & Neff, J. C. (2005). Radiative effects of desert dust deposits to alpine snow. *Eos Trans. AGU, 86*(52), Fall Meet. Suppl., Abstract B34B-05. Retrieved from https://ui.adsabs.harvard.edu/abs/ 2005AGUFM.B34B..05P/abstract

Pelto, M. (2004). *Temperature-ablation relationships on glaciers and in alpine areas, North Cascades, Washington.* In Proc. Eastern Snow Conf., 61 (135–145).

Pepe, M., Brivio, P. A., Rampini, A., Rotanodari, F., & Boschetti, M. (2005). Snow cover monitoring in Alpine regions using ENVISAT optical data. *International Journal of Remote Sensing*, *26,* 4661–4667.

Pielke, R. A. (2005). Land use and climate change. *Science*, *310*(5754), 1625–1626. doi: 10.1126/science.1120529.

Pielmeier, C., & Schneebeli, M. (2003). Developments in the stratigraphy of snow. *Survey Geophysics, 24*(5–6)*,* 389–416. doi: https://doi.org/10.1023/B:GEOP.0000006073.25155.b0.

Pirazzini, R., Raisanen, P., Vihma, T., Johansson, M., & Tastula, E. M. (2015). Measurement and modelling of snow particle size and shortwave infrared albedo over a melting Antartica ice sheet. *The Cryosphere, 9,* 2357 – 2381. doi: 10.5194/tc-9-2357-2015.

Pishva, D. (2011). Use of spectral biometrics for aliveness detection. In G. Chetty (Ed.), *Advanced biometric technologies.* doi: 10.5772/17100.

Pizarro, R. (1967). *Estimation of incoming radiation from extraterrestrial radiation and climatic data* [Master's thesis]. Utah State University, Logan, Utah. Retrieved from https://digitalcommons.usu.edu/etd

Pomeroy, J. W., de Boer, D., & Martz, L. W. (2007). Hydrology and water resources. In B. Thraves et al. (Eds.), *Saskatchewan: Geographic perspectives, Canadian Plains Res. Cent.* (63-80). Regina, Canada. Retrieved from https://www.researchgate.net/publication/292409837

Pomeroy, J. W., & Brun, E. (2001). Physical properties of snow. In H. G. Jones, J. W. Pomeroy, D. A. Walker, & R. W. Homan (Eds.), *Snow ecology* (45-126). Cambridge University Press, Cambridge.

Pomeroy, J. W., & Jones, H. G. (1996). Wind-blown snow: Sublimation, transport and changes to polar snow. In E. W. Wol, & R. C. Bales (Eds.), *Chemical exchange between the atmosphere and polar snow, NATO ASI Series I,* 43 (453-490). Springer-Verlag, Berlin.

Prata, A. J. (1996). A new long-wave formula for estimating downward clear-sky radiation at the surface. In Q. J. Roy (Ed.), *Met. Soc., 122,* 1127 – 1151.

Pruppacher, H. R., & Klett, J. D. (1996). *Microphysics of clouds and precipitation.* Kluwer Academic Publishers.

Raes, D. (2009). The ETo calculator. Reference manual version 3.1. *Food and Agriculture Organization of the United Nations.* Rome, Italy. Retrieved from http://www.fao.org/fileadmin/user_upload/faowater/docs/ReferenceManualETo.pdf

Raleigh, M. S., Landry, C. C., Hayashi, M., Quinton, W. L., & Lundquist, J. D. (2013). Approximating snow surface temperature from standard temperature and humidity data: New possibilities for snow model and remote sensing evaluation. *Water Resources Research, 49,* 8054 – 8069. doi: 10.1002/2013WR013958, 2013

Rango, A. (1980). Operational applications of satellite snow cover observations. *Journal of American Water Resources Association, 16,* 1066–1073. doi:10.1111/j.1752-1688.1980.tb02549.x.

Rasmus, S. (2005). *Snow pack structure characteristics in Finland—Measurements and modelling* [Doctoral dissertation]. University of Helsinki.

Rasmus, S., Kivinen, S., & Irannezhad, M. (2018). Basal ice formation in snow cover in Northern Finland between 1948 and 2016. *Environmental Research Letters,13*(11), 114009. doi: https://doi.org/10.1088/1748-9326/aae541.

RDG Planning & Design and Applied Ecological Services. (May, 2012). Comprehensive Plan for the City of Cedar Falls. Retrieved from http://www.cedarfalls.com/DocumentCenter/View/2418/2012-Cedar-Falls-Comprehensive-Plan?bidId=

Rennert, K. J., Roe, G., Putkonen, J., & Bitz, C. M. (2009). Soil thermal and ecological impacts of rain on snow events in the circumpolar Arctic. *J. Clim., 22,* 2302–2315.

Rice, R., Painter, T., & Dozier, J. (2007). *Snow cover along elevation gradients in the Upper Merced and Tuolumne river basins of the Sierra Nevada of California from MODIS and blended ground data.* 75th Western Snow Conference, 3–12.

Rico, M., Benito, G., Salgueiro, A. R., Díez-Herrero, A., & Pereira, H. G. (2008). Reported tailings dam failures: A review of the European incidents in the worldwide context. *J. Hazard. Mater., 152*(2), 846–852. doi:10.1016/j.jhazmat.2007.07.050.

Richards, J. A. (1999). Remote sensing digital image analysis. *Springer-Verlag,* 1-240. Berlin, Germany. doi: https://doi.org/10.1007/978-3-662-03978-6.

Riihelä, A., Lahtinen, P. & Hakala, T. (2011). The radiation snow characteristics and albedo at summit. *RASCAL Expedition Report, 8,* 1-46. Finnish Meteorological Institute.

Rindfuss, R. R., Walsh, S. J., Turner, B. L., II, Fox, J., & Mishra, V. (2004). Developing a science of land change: Challenges and methodological issues. *Proc. Natl. Acad. Sci., 101*(13976–13981).

Rinnen, S., Stroth, C., Riße, A., Henning, C. O., & Arlinghaus, H. F. (2015). Characterization and identification of minerals in rocks by ToF-SIMS and principal component analysis. *Applied Surface Science, 349,* 622-628. doi: https://doi.org/10.1016/j.apsusc.2015.04.231

Riseborough, D., Shiklomanov, N., Etzelmuller, B., Gruber, S., & Marchenko, S. (2008). Recent advances in permafrost modelling. *Permafr. Periglac. Processes, 19,* 137–156.

Roebber, P. J., Bruening, S. L., Schultz, D. M., & Cortinas, J. V. (2003). Improving snowfall forecasting by diagnosing snow density. *Weather and Forecasting, 18*(2), 264 – 287.

Robinson, D. A., Dewey, K. F., & Heim, R. R. (1993). Global snow cover monitoring: An update. *Bulletin of the American Meteorological Society, 74*(9), 1689-1696. doi: https://doi.org/10.1175/1520-0477(1993)074<1689:GSCMAU>2.0.CO;2

Ruffieux, D. (1995). Winter surface energy budget in Denver, Colorado. *Atmospheric Environment, 10*(13), 1579 – 1587. Elsevier.

Saha, A., Garg, P. K., & Patil, M. (2019). The effect of contaminated snow reflectance using hyperspectral remote sensing – a review. *International Journal of Image and data fusion, 10*(2), 107 - 130. doi. https://doi.org/10.1080/19479832.2019.1582561.

Salisbury, N. E., & Honey, R. D. (2019). Iowa. In *Encyclopaedia Britannica.* Retrieved from, https://www.britannica.com/place/Iowa-state

Salisbury, J. (1998). Spectral measurement field guide. In *Defence Technology Information* (Center Report ADA362372). Retrieved from http://www.dpinstruments.com/papers/spectral_guide.pdf

Schmid, A. O., Gulbel, S., FIddes, J., & Gruber, S. (2012). Inferring snowpack ripening and melt-out from distributed measurements of near-surface ground temperatures. *The Cryosphere, 6,* 1127–1139. doi: 10.5194/tc-6-1127-2027-2012

Schultz, G. A., & Barrett, E. C. (1989). Advances in remote sensing for hydrology and water resources management. *Technical Document In Hydrology, UNESCO, 102.*

Schweizer, J., Jamieson, J. B., & Schneebeli, M. (2003). Snow avalanche formation. *Rev. Geophys., 41*(4). doi:10.1029/2002RG000123.

Seibert, J., Jenicek, M., Huss, M., & Ewen, T. (2015). Snow and Ice in Hydrosphere. *Snow and ice-related hazards, risks, and disasters,* 99 – 137. doi: 10.1016/B978-0-12-394849-6.00004-4

Seidel, F. C., Rittger, K., Skiles, S. M., Noah P. Molotch, N. P., & Painter, T. H. (2016). Case study of spatial and temporal variability of snow cover, grain size, albedo and radiative forcing in the Sierra Nevada and Rocky Mountain snowpack derived from imaging spectroscopy. *The Cryosphere, 10,* 1229–1244. Retrieved from www.the-cryosphere.net/10/1229/2016/.

Sensoy, A., Sorman, A. A., Tekeli, A. E., Sorman, A. U., & Garen, D. C. (2006). Point-scale energy and mass balance snowpack simulations in the upper Karasu basin, Turkey. *Hydrological Processes, 20,* 899-922. doi: https://*doi*.org/10.1002/hyp.6120.

Serreze, M. C., Barrett, A. P., Stroeve, J. C., Kindig, D. N., & Holland, M. M. (2009). The emergence of surface-based Arctic amplification. *Cryosphere, 3,* 11–19.

Singh, S. K., Kulkarni, A. V., & Chaudhary, B. S. (2010). Hyperspectral analysis of snow reflectance to understand the effects of contamination and grain size. *Annals of Glaciology, 51*(54), 83-88.

Singh, S. K., Negi, H. S., Raj, B G. K., Kulkarni, A. V., & Sharma, J. K. (2005). Spectral reflectance investigation of snow and other objects using ASD spectroradiometer. *Report RSAM/SAC/RESIPA/MWRG-GLI/SN 23 /2005.* doi: 10.13140/RG.2.2.29730.84166

Steckly, S. R. (2006). Soil survey of Black Hawk County, Iowa. In *United States Department of Agriculture, Natural Resources Conservation Service.* Washington, D.C. Retrieved from http://purl.access.gpo.gov/GPO/LPS76863

Stewart, I. T. (2009). Changes in snowpack and snowmelt runoff for key mountain regions. *Hydrol. Processes, 23,* 78–94.

Stoelinga, M., Woods, C. P., Locatelli, J. D., & Hobbs, P. V. (2005, June). *On the representation of snow in bulk microphysical parameterization schemes.* In Proceedings of the WRF/MM5 User's Workshop, Boulder, CO.

Sturm, M., & Holmgren, J. (1995). Seasonal snow cover classification system for local to global applications. *J. Climate*, *8,* 1261–1283. Retrieved from https://doi.org/10.1175/1520-0442(1995)008<1261:ASSCCS>2.0.CO;2

Sui, J., & Koehler, G. (2001). Rain-on-snow induced flood events in Southern Germany. *Journal of Hydrology, 252,* 205– 220.

Tarboton, D. G., Chowdhury, T. G., & Jackson, T. H. (1995). *A spatially distributed energy balance snowmelt model.* In Proceedings of symposium on biogeochemistry of seasonally snow-covered catchments, Boulder, Colorado.

Thenkabail, P. S., Enclona, E. A., Ashton, M. S., & Van Der Meer, B. (2004). Accuracy assessments of hyperspectral waveband performance for vegetation analysis applications. *Remote Sens. Environ., 91*, 354-376.

Trajkovic, S., Stojnic, V., & Gocic, M. (2011). Minimum weather data requirements for estimating reference evapotranspiration. *Architecture and Civil Engineering, 9*(2), 335 – 345.

Tsai, F., Lin, E. K., & Yoshino, K. (2007). Spectrally segmented principal component analysis of hyperspectral imagery for mapping invasive plant species. *International Journal of Remote Sensing, 28*(5)*, 1023-1039

Upadhayay, D. S., Rajnikant, Chowdhury, J. N., & Katyal, K. N. (1985). Some characteristics of snow cover in upper Beas Catchment. *Mausam, 36*(2), 215–220.

US Army Corps of Engineers. (1998). *Runoff from snowmelt* (EM 1110-2-1406). Washington, DC, USA.

U.S. Army Corps of Engineers. (1956). *Snow hydrology: Summary report of the snow investigations of the North Pacific Division.* In North Pacific Division, Corps of Engineers, US Army, (437), Portland, OR, USA.

U.S. Census Bureau. Retrieved from http://www.census.gov/quickfacts/table/ PST045215/19013.

Usul, N., & Turan, B. (2006). Flood forecasting and analysis within the Ulus Basin, Turkey, using geographic information systems. *Natural Hazards, 39,* 213–229. doi: 10.1007/s11069-006-0024-8

Vikhamar, D., & Solberg, R. (2003). Snow-cover mapping in forests by constrained linear spectral unmixing of MODIS data. *Remote Sensing of Environment, 88,* 309–323.

Villa, A., Chanussot, J., Benediktsson, J. A., & Jutten, C. (2011). Spectral unmixing for the classification of Hyperspectral Images at a finer spatial resolution. *IEEE Geosci. Remote Sensing. Lett., 8*(4), 760-764. doi: https://doi.org/10.1109/ JSTSP2010.2096798.

Warren, S. G. (1982). Optical properties of Snow. *Review of Geophysics and space physics, 20*(1)*, 67-89.

Weismüller, J., Wollschläger, U., Boike, J., Pan, X., Yu, Q., & Roth, K. (2011). Modeling the thermal dynamics of the active layer at two contrasting permafrost sites on Svalbard and on the Tibetan Plateau. *Cryosphere, 5,* 741–757.

Wen, H., Wen-shou., W., Ming-zhe, L., Heng, L., Xi, H., & Yan-wei, Z. (2014). Metamorphism and microstructure of seasonal snow: Single layer tracking in western Tianshan, China. *Journal of Mountain Science, 11*(2)*,* 496-506. doi: 10.1007/s11629-013-2815-1.

Willis, I. C., Arnold, N. S., & Brock, B. W. (2002). Effect of snow pack removal on energy balance, melt and runoff in a small supraglacial catchment. *Hydrological Processes, 16,* 2721–2749. doi:10.1002/hyp.1067.

Wiscombe, W. J., & Warren, S. G. (1980). A model for the spectral albedo of snow—I: Pure snow. *Journal of Atmospheric Sciences, 37,* 2712–2733.

Ye, X., Sakai, K., Okamoto, H., & Garciano, L. O. (2008). A ground-based hyperspectral imaging system for characterizing vegetation spectral features. *Computers and Electronics in Agriculture, 63*(1), 13–21

You, J. (2004). *Snow hydrology: the parameterization of subgrid processes within a physically based snow energy and mass balance model* [Doctoral dissertation]. Utah State University, USA.

Zanotti, F., Endorzzi, S., Bertoldi, G., & Rigon, R. (2004). *The GEOTOP snow model*. 61st Eastern Snow Conference Portland, Maine, USA.

Zeinivand, H., & de Smedt, F. (2009). Prediction of snow floods with a distributed hydrological model using a physical snow mass and energy balance approach. *Natural Hazards, 54,* 451 – 468. doi. 10.1007/s11069-009-9478-9

Zeleke, G., & Hurni, H. (2001). Implications of land use and land cover dynamics for mountain resource degradation in the Northwestern Ethiopian highlands. *Mt. Res. Dev., 21* (2), 184–192.

Zhang Y., Xiao Q., Wen J., et al. (2017). Review on spectral libraries: Progress and application. *Journal of Remote Sensing, 21*(1), 12-26.

Zhao, H., & Fernandes, R. (2009). Daily snow cover estimation from Advanced Very High Resolution Radiometer Polar Pathfinder data over Northern Hemisphere land surfaces during 1982–2004. *Journal of Geophysical Research*, *114,* 1–14.

Zhao, S., Jiang, T., & Wang, Z. (2013). Snow grain-size estimation using Hyperion Imagery in a typical area of the Heihe River Basin, China. *Remote Sensing, 5,* 238-253, ISSN 2072-4292. doi: https://doi.org/10.3390/rs5010238.

Zhong, X., Zhang, T., Kang, S., Wang, K., Zheng, L., Hu, Y., & Wang, H. (2018). Spatiotemporal variability of snow depth across the Eurasian continent from 1966 to 2012. *The Cryosphere, 12,* 227–245. doi: https://doi.org/10.5194/tc-12-227-2018, 2018.

APPENDIX

NOTATION

ΔQ= Net energy at the surface (W m^{-2})
Sin =Incoming shortwave radiation (W m$^{-2)}$
Sout =Outgoing fluxes of shortwave (W m^{-2})
Lin= Incoming long-wave radiation (W m^{-2})
Lout= Outgoing long-wave radiation (W m^{-2})
Hse= Sensible heat flux (W m^{-2})
Hla =Latent heat flux (W m^{-2})
Es= Emissivity of the snow surface (0.97)
σ =Stefan Boltzmann constant (5.67 $\times 10-8$W m^{-2} K^{-1})
Ta =Air temperature (°C)
Ts= Snow surface temperature (°C)
ρa Air density (1.2922 kg m^{-3} at standard temperature and pressure)
ρs =Density of snow (kg m^{-3})
Ua =Wind velocity (m/s)
L =Latent heat of sublimation (2.834 $\times 106$ J kg^{-1} at 273.15K)
Lf =Latent heat of fusion (3.335 $\times$ 105 J kg^{-1})
Pa =Atmospheric pressure (mb)
Mv Molecular weight of water vapour (18.015 $\times$ 10^{-3} kg mol^{-1})
Ma =Molecular weight of dry air (28.96 $\times$ 10^{-3} kg mol^{-1})
Ei =Saturation vapour pressure (mb)
Ri =Richardson number (= 0 for neutral and < 0 for unstable, > 0 for stable)
Ch =Heat transfer coefficient (1.0 $\times$ 10^{-4} $-1.08 \times$ 10^{-2})
Ce =Humidity transfer coefficient (1.0$\times$10^{-4}$-$ 1.08 $\times$ 10^{-2})
dm =Amount of snow-melt (mm of water/day)
c =Specific heat of snow (2.211 $\times$ 103 J kg^{-1} K^{-1})
Ca= Specific heat of air (1.006 $\times$ 103 J kg^{-1} K^{-1})